

**Final Report**  
of  
**Major Research Project**  
of  
**University Grant Commission, New Delhi**  
[ File No. 39 - 509 / 2010 (SR), 04 - 01 - 2011  
w. e. f. February 01, 2011]  
**in Physics**  
**Project Entitled**  
**Study of Photonic Band gap Materials for the use of Broadband Microwave  
Antenna**  
Submitted By  
**DR. PRAKASH NAYAK**  
PRINCIPAL INVESTIGATOR  
ASSOCIATE PROFESSOR  
H. O. D. PHYSICS  
R. K. College  
(Under Lalit Narayan Mithila University, Darbhanga)  
MADHUBANI ( BIHAR ) 847211  
INDIA  
**2014**

## **CERTIFICATE**

I, Dr. Prakash Nayak, Ph. D., declare that the work presented in this report is original and carried out throughout independently by me during the complete tenure of Major Research Project of U. G. C., New Delhi.

*Prakash Nayak*  
**DR. PRAKASH NAYAK**

PRINCIPAL INVESTIGATOR

ASSOCIATE PROFESSOR

H. O. D. PHYSICS

R. K. College

(Under Lalit Narayan Mithila University,  
Darbhanga)

MADHUBANI ( BIHAR ) 847211

INDIA

[Prakashnayak.17@gmail.com](mailto:Prakashnayak.17@gmail.com)

## Acknowledgment

I feel greatly indebted to the University Grant Commission, New Delhi for the award of Major Research Project and the financial assistance to pursue the research project. I convey my sincere thanks to the authorities of R. K. College, Madhubani for providing basics infrastructure facilities in the department of Physics to carry out the project. I also feel indebted to the project fellow Dr. Dhirendra Kumar. M. Sc., Ph. D. for not only sincerely supporting the research work but also taking active part in resolving technical issues involved in research work.

*Prakash Nayak*

**DR. PRAKASH NAYAK**

Principal Investigator

Associate Professor

Department of Physics

R. K. College

Madhubani ( Bihar ) 847211

India

[Prakashnayak.17@gmail.com](mailto:Prakashnayak.17@gmail.com)

## **SUMMARY OF FINAL REPORT**

**of**

**Major Research Project of UGC, New Delhi**

**[ F. No. 39 - 509 / 2010 ( SR ) dated 04 - 01 - 2011 ]**

**In**

**Physics entitled**

**Study of Photonic Band Gap Materials for the use of Broadband Microwave Antenna**

The whole work initiated and completed may be divided into three sections

**Section 1.** Review work based on Proposed Problem.

**Section 2.** Analytical methods / techniques used in the study of PBG structures for antenna applications

**Section 3.** Study of the effect of PBG Structures on the performance of microwave antenna

### **Section 1**

At the pre and initial stages of the project intensive literature survey based on microstrip and printed antenna, relative permittivity of substrate and substrate height, PBG Structure as antenna substrate devoted to develop new design to improve antenna bandwidth along with other figure of merits were carried out in a planned manner. Five review papers were prepared over these topics and all were published in different journals. The details are mentioned as under

**Paper 1.** "Theoretical Study of Multi Band Microstrip Antenna"

Published in **Bulletin of Pure and Applied Physics, Vol. 28 D, No. 1, pp. 13 - 19, 2009**

**Paper 2.** "Analysis of Dielectric Lens Antenna for Microwave Radiation Detector"

Published in **Indian Journal of Physical Science, Vol. 1, No. 1, PP. 55 – 58, 2009.**

**Paper 3.** “ Integrated E - Shape and H - Shape Broadband Microstrip Patch Antenna”

Published in **Acta Ciencia Indica, Vol. XXXVI, No. 2, pp. 297 – 300, 2010.**

**Paper 4.** “ Effect of Substrate Height on Compact Broadband Microstrip Patch Antenna”

Published in **Indian Journal of Theoretical Physics, Vol. 8, No. 3, pp. 203 - 207, 2010.**

**Paper 5.** “ Study of Effect of Shorting Wall length for Designing a Compact Circularly Polarised Microstrip Patch Antenna ”.

Published in **Indian Journal of Theoretical Physics, Vol. 60, No. 2, pp. 93-99. 2012.**

## **Section 2**

A common property of most microstrip antennas is that the element launches surface wave mode, in addition to the field radiated in space. For finite – size substrate, the surface wave power will diffract from the edges of the substrate, resulting in disturbance of the radiating pattern. The excitation of the surface waves also result in increased mutual coupling between antenna elements. Suppressing or reduction of surface waves will naturally improve antenna efficiency and cause reduction in side lobe level.

Use of photonic crystal (PC) as antenna substrate can offer a real solution to the surface wave problem. PCs are a class of periodic metallic, dielectric or composite structures that exhibits pass and stop bands in their frequency response. Because of this they offer the property to forbid the propagation of electromagnetic waves whose frequency is included within their stop band – so called Photonic Band Gap (PBG). Hence if the substrate periodically loaded to create a PBG crystal in such a way that the frequency of the substrate mode overlaps the stop band frequency of the crystal, the excited substrate mode

exponentially decays thus reducing the energy lost into the substrate. Thus an increased amount of radiated power couples to space waves and this mechanism will have the effect of reshaping the antenna pattern.

From solid state theory, we know that semiconductors allow electron conduction without scattering only for electrons that have energies within a specific range of energy, often termed band – gaps. Electromagnetic wave propagation in periodic dielectric media is analogue to electron – wave propagation in semiconductor crystals. Although fundamentally different mechanism are involved, preliminary results suggest that at microwave and millimetre wave frequencies the propagation characteristics of these crystals can be manipulated by carefully designing and fabricating structures composed of regions of differing dielectric constants.

Recent developments in computational electromagnetic (CEM) methods including finite elements (FE) method, finite difference time domain (FDTD) method, finite difference frequency domain (FDFD) method, the transmission line matrix (TLM) and method of moments (MoM) solutions have added significantly to the toolbox of physicists and engineers alike. With the advent of general purpose electromagnetic (EM) codes, a novel solution has been introduced to the technical community, simulation.

In our work, we mostly make use of

**A. Finite – difference – time – domain (FDTD) numerical analysis technique**

Since it is a time- domain – method, FDTD solutions can cover a wide frequency range with a single simulation run. The time dependent Maxwell's equations are discretized using central difference approximations to the space and time partial derivatives. The resulting finite difference equations are solved in software. The electric field vector components in a volume space are solved in given instant of time; then the magnetic field vector components in the same spatial volumes are solved at the next instant in time and the process is repeated over and over again until the desired transient or steady is fully evolved.

To implement an FDTD solutions of Maxwell's equation, a computational domain first is established over which simulation is performed to determine E and H fields at every point in the space within that computational domain. Computational domain could be any materials whose permeability, permittivity and conductivity are specified.

### **B. High frequency Structure Simulator (HFSS) for Antenna Simulation**

HFSS for antenna simulation is a valuable tool in antenna design because of its ability to virtually design and evaluate what if scenarios. Basic performance characteristics such as return loss, input impedance, gain, directivity and a variety of polarisations characteristics can be analysed in HFSS. Its ability to overlay 3D field pattern on antenna geometry provide invaluable insight and direct correlation between the antenna and resulting radiation pattern. HFSS also offers electric and magnetic field visualisation both in the near – field and far – field providing design understanding that is not easily available through measurement. With multiple advanced solver techniques to simulate, not just the antenna but also the effect of its interactions with the entire system, including the feeding system as well as the platform, HFSS is invaluable tool not only in antenna design but placement as well.

## **Section 3 (Application Part)**

**Paper 6.** “ Transforming Maxwell's Equations into Equivalent Schrodinger Equation for the Photonic Band Gap Structures ”

In this paper in analogy with Kronig – Penney model for electronic band – gaps in periodic potentials. Maxwell's equations for the propagation of light in the photonic crystals are transformed into an equivalent form of Schrödinger's equation. The propagation of electromagnetic wave through doped semiconductor is well represented by a frequency dependent Drude model.

Published in **Acta Ciencia Indica, Vol. XXXVIII, No. 4, PP. 275 – 280, 2012.**

**Paper 7.** “ Analysis of Surface Wave Propagation in PBG Structure ”

In this paper surface wave propagation along the planar PBG lattice has been investigated. Two dielectric slabs clad with the planar PBG structures – one on

a conductor backed slab and the other on a bare dielectric slab were used. The first TM – lattice mode has a cut – off frequency at the X – point of 11.4 GHz for the case of planar PBG on a bare dielectric slab and 8.4 GHz for the case of planar PBG on a conductor backed dielectric slab.

**Under Consideration for publication in Acta Ciencia Indica.**

**Paper 8.** " Study of the Effect of PBG Structure on the Performance of Printed Antenna"

In this paper it has been shown by simulated results that performance of printed array antenna is significantly improved by using a photonic band Gap (PBG) substrate instead of standard substrate. As a first steps towards realization of an array antenna two printed spirals have been put next to each other and simulation have been made with or without PBG structures. The improvement on the radiation pattern caused by the presence of PBG structure was found to be significant.

**Accepted and abstract published in Physical Sconces Section – ISCA 2013.**

**Paper 9.** " Photonic Crystals as a substrate for Patch Antenna "

In this paper the design of a photonic crystal as substrate for patch antenna is discussed. Simulation results with HFSS software showed significant reduction in frequency dependence of the radiation pattern when photonic crystals are used as substrate. At the design frequency, the patch antenna on a photonic crystal has more directivity, less side back radiation and a smoother pattern. The gain in bore sight directions increases significantly. This opens the door to design new devices with thicker substrates of higher dielectric without losing performance by the undesired excitations of the surface wave modes.

Published in **Physical and Environmental Science Bulletin, Vol. 1, No. 2, pp. 35 – 38, 2013.**

**Paper 10.** " State of Research on Using PBG Components in Radio Frequency Antenna System "

In this paper a brief survey of a recent trends and developments of radio frequency (RF) antenna oriented PBG research beginning with the use of PBG substrate for planar antenna and concluding with an examination of PBG

structures as antenna reflector is presented. More research to resolve question concerning both the effect of a PBG substrate on an antenna's pattern shape and the sensitivity of antenna performance to placement relative to PBG lattice have been suggested.

**Accepted for publication in journal of Chemistry and Chemical Engineering, ISSN 1934 – 737, paper No. JCHF – E 203083002.**

**Paper 11.** "Study of Pattern and Gain Properties of Dipole Antenna"

In this paper the pattern, gain and impedance properties of a dipole antenna located close to PBG screen as a high impedance conductor to act as an antenna ground plane or screen were examined. The advantage was that such a surface, with a reflection coefficient of +1 instead of -1 produced by an electric conductor, would allow a dipole parallel to the surface to be placed close to it. Investigation were made specifically how do the broadside directivity, pattern and impedance of a half – wave dipole parallel to the surface vary with the reflection phase angle.

Published in **Physical and Environmental Science Bulletin, Vol. 2, No. 1, pp. 39 – 40, 2014.**

**Paper 12.** "Study of Photonic Band Gap Structures below Infrared Wavelengths"

In this paper we have been able to show that for two – dimensional square and triangular lattices have in – plane complete photonic bandgaps (CPBGs) below infrared wavelengths. The optimal one for ideal Drude – like behaviour is a square lattice, whereas for Drude – like behaviour in silver, the geometry is triangular lattice. If the lattice spacing is tuned to a characteristic plasma wavelengths, several CPBGs open in the spectrum and their relative gap width can be large. Such structures can provide CPBG structures with bandgaps down to ultraviolet wavelengths.

Published in **Physical and Environmental Science Bulletin, Vol. 2, No. 2, pp. 9 – 62, 2014.**

## Contents

Paper Sr. No	Title of Paper	Published In
1.	Theoretical Study of Multi Band Microstrip Antenna	Bulletin of Pure and Applied Physics, Vol. 28 D, No. 1, pp. 13 – 19, 2009.
2.	Analysis of Dielectric Lens Antenna for Microwave Radiation Detector	Indian Journal of Physical Science, Vol. 1. No. 1, PP. 55 - 58, 2009.
3..	Integrated E – Shape and H – Shape Broadband Microstrip Patch Antenna	Acta Ciencia Indica, Vol. XXXVI, No. 2, pp. 297 – 300, 2010
4.	Effect of Substrate Height on Compact Broadband Microstrip Patch Antenna	Indian Journal of Theoretical Physics, Vol. 8, No. 3, pp. 203 – 207, 2010.
5.	Study of Effect of Shorting Wall length for Designing a Compact Circularly Polarised Microstrip Patch Antenna	Indian Journal of Theoretical Physics, Vol. 60, No. 2, pp. 93-99. 2012.
6.	Transforming Maxwell's Equations into Equivalent Schrodinger Equation for the Photonic Band Gap Structures	Acta Ciencia Indica, Vol. XXXVIII, No. 4, PP. 275 – 280, 2012.
7.	Analysis of Surface Wave Propagation in PBG Structure	Under Consideration for publication in Acta Ciencia Indica
8.	Study of the Effect of PBG Structure on the Performance of Printed Antenna	Accepted and abstract published in Physical Sciences Section – ISCA 2013
9.	Photonic Crystals as a substrate for Patch Antenna	Physical and Environmental Science Bulletin, Vol. 1, No. 2, pp. 35 – 38, 2013.
10.	State of Research on Using PBG Components in Radio Frequency Antenna System	Accepted for publication in journal of Chemistry and Chemical Engineering (International Standard Serial; Number ISSN 1934 – 737, paper No. JCHF – E 203083002
11.	Study of Pattern and Gain Properties	Physical and Environmental

	of Dipole Antenna	Science Bulletin , Vol. 2, No. 1, pp. 39 – 40, 2014.
<b>12.</b>	Study of Photonic Band Gap Structures below Infrared Wavelengths	Physical and Environmental Science Bulletin, Vol. 2, No. 2, pp. 59 – 62, 2014

Complete Statistics of Work presented in the Final Report

Published ----- 10

Accepted ----- 01

Under Consideration ----- 01

**Total** ----- **12.**

## THEORETICAL STUDY OF MULTI-BAND MICROSTRIP ANTENNA

Dhirendra Kumar\*, Prakash Nayak\*\* and Lalan jha\*\*\*

\* Department of Physics, Mithila Janta Inter College, Madhubani-847211 (Bihar)

### ABSTRACT

In the present paper on the basis of concept of inserting slot arrays following a known antenna distribution a theoretical study of a multi-wideband microstrip-patch antenna has been made. The design of antenna included the insertion of rectangular slots following a Chebyshev distribution around a central rectangular slot in addition to a triangular slot. These slots engraved in rectangular and triangular patch are joined together and fed by one probe feed. A close agreement was found when theoretical results were compared with simulated results.

**Key words :** Microstrip antennas, Multifrequency antennas, Wideband antennas.

### INTRODUCTION

With the growing demand of modern wireless communication there has been significant surge in researches leading to novel design and application of various type of antenna. To achieve various functionalities, such as dual frequency operation, dual band circular polarised performance polarisation diversity with only one patch and a single feed a reconfigurable patch antenna with switchable slots (PASS) was proposed (Sittironnarit and Ali,2002). For wireless local area network applications a dual wideband folded microstrip patch antenna was introduced (Yang and Rahmat-Samii,2003). For the design of dual-band microstrip antenna a cavity-model based simulation tools, along with genetic optimization algorithm was presented in Ozlem *et al* (2003). Multiple slots in the patch, or multiple shorting strips between the patch and the ground plane have been used. Acceptable antenna operation over the desired frequency band was then achieved by optimization of the position of the slots and performance of shorting strips via a genetic optimization algorithm. Using similar approach a single low-profile printed antenna which provided dual-band operation by having loading from two-step slots embedded close to radiating edge was presented in Khairul *et al* (2003) . It has been suggested in Khairul *et al* (2003) that the ratio of the two frequencies can be well controlled by the aspect ratio of the step-loading dimension.

---

\*\* P.G. Department of Physics, R.K.College, Madhubani-847211 (Bihar)

\*\*\*University Department of Physics, L.N.M.University, Darbhanga-846004 (Bihar)

In this paper a multi-band antenna design approach based on inserting rectangular slots, following a Chebyshev distribution, in addition to a triangular slots into the patch, which represents a combination of a rectangular and isosceles-triangular patch have been presented. The sample antenna was simulated and compared with theoretical results. There was good agreement between the theoretical and simulated results.

#### ANTENNA GEOMETRY AND RADIATION PATTERN OF THE PROBLEM

The proposed antenna geometry is based on joining a rectangular patch and a triangular patch, in order to increase the radiation area, as shown in Figure 1. The structure is fed by a  $50\Omega$  coaxial probe. The radiation pattern of the proposed structure with this feeding technique is determined by adding the fields radiated by the rectangular patch to those radiated by the triangular patch. The substrate used in the formulation process was of thickness  $h = 0.32$  cm. The far electric fields of the rectangular patch were given in Balanis,(1997) as

$$E_\theta = \frac{K e^{jk_0 r}}{r} \cos(k_0 h \sqrt{\epsilon_r} \cos\theta) \frac{\sin\left(\frac{\pi W}{\lambda_0} \sin\theta \sin\varphi\right) \cos\left(\frac{\pi L}{\lambda_0} \sin\theta \cos\varphi\right) \cos\varphi}{\sin\theta \sin\varphi} \quad (1)$$

$$E_\varphi = \frac{-K e^{jk_0 r}}{r} \cos(k_0 h \sqrt{\epsilon_r} \cos\theta) \frac{\sin\left(\frac{\pi W}{\lambda_0} \sin\theta \sin\varphi\right) \cos\left(\frac{\pi L}{\lambda_0} \sin\theta \cos\varphi\right) \cos\theta}{\sin\theta \sin\varphi} \quad (2)$$

In Equations (1) and (2),  $k_0$  is the wavenumber,  $\lambda_0$  is the wave-length,  $\epsilon_r$  is the dielectric permittivity, and  $W$  and  $L$  are the width and the length dimensions of the rectangular patch, respectively. The far electric fields radiated from an equilateral triangle were given in Lee *et al* (1988) as

$$E_\theta = -j\omega\eta_0 (F_x \cos\theta \cos\varphi + F_y \cos\theta \sin\varphi) \quad (3)$$

$$E_\varphi = -j\omega\eta_0 (-F_x \sin\varphi + F_y \cos\varphi) \quad (4)$$

In Equations (3) and (4),  $\eta_0 = 120\pi \Omega$ , and the terms  $F_x$  and  $F_y$  are the electric potential components. These were given in detail in Lee *et al* (1988) ,

## THEORETICAL STUDY OF MULTI-BAND MICROSTRIP ANTENNA

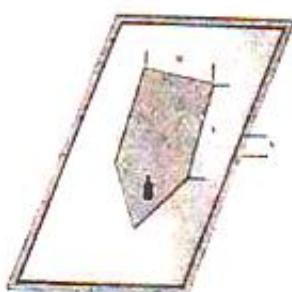


Figure 1 : A rectangle added to an equilateral triangle patch, fed by a probe.

By specifying the lowest-order mode, TM010, for approximating the rectangular dimensions to a length,  $L$ , of 4 cm and width,  $W$ , of 3 cm, and for an equilateral triangle 3 cm on a side, for an operating frequency,  $f_0$ , of 3.24 GHz, Equations (1) and (2) become

$$E_\theta = \frac{Ke^{-jk_0 r}}{r} \cos(0.322 \cos\theta) \frac{\sin(0.9448 \sin\theta \sin\varphi) \cos(0.7086 \sin\theta \cos\varphi)}{\sin\theta \sin\varphi} \cos\theta \quad (5)$$

$$E_\varphi = \frac{Ke^{-jk_0 r}}{r} \cos(0.322 \cos\theta) \frac{\sin(0.9448 \sin\theta \cos\varphi) \cos(0.7086 \sin\theta \cos\varphi)}{\sin\theta} \cos\theta \quad (6)$$

It is clear from Equation (5) that for  $\varphi = 0^\circ$  and  $\varphi = 90^\circ$ , both components of the electric field vanish, due to the terms  $\sin\varphi$  and  $\cos\varphi$ , respectively. Moreover, for  $\varphi = 90^\circ$ , Equation (6) becomes

$$E_\varphi = \frac{Ke^{-jk_0 r}}{r} \cos(0.322 \cos\theta) \frac{\sin(0.9448 \sin\theta)}{\sin\theta} \cos\theta \quad (7)$$

For an equilateral triangular patch, the  $\varphi$  components of the electric field are given by the product of the terms  $A$  and  $C$ , given by

$$A = \left\{ \frac{2j(139.6258 + j39.1789 \sin \theta [\sin(1.01789 \sin \theta)])}{6498.455 - 1534.986 \sin^2 \theta} \right. \\ \left. + \frac{2j \cos(1.01789 \sin \theta) - 2j}{39.1789 \sin \theta} \right\}. \quad (8)$$

$$C = -j\omega \eta_0 [(4\pi r)^{-1} \epsilon_0^{-1} h e^{jk_0 r}] e^{j39.1789 \sin \theta \cos \varphi} 2j\omega \mu C_{01} \quad (9)$$

$C_{01}$  is constant defined in Lee *et al* (1988). The total electric field of the new structure is obtained by adding the electric field radiated from the rectangular patch, defined in Equation (7), to that of the triangular patch, derived in Equations (8) and (9). A comparison between calculated and simulated results is shown in Figure 2 (a & b).

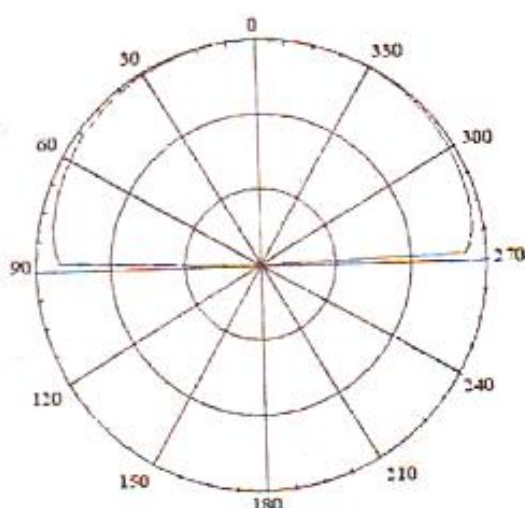


Figure 2a. The simulated electric field, to be compared to Fig. 2b.

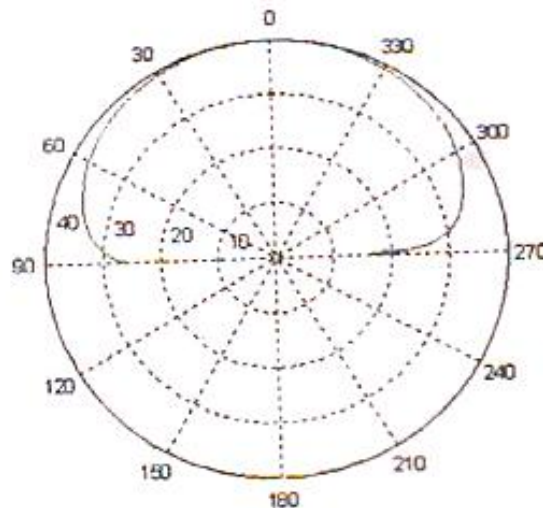


Figure 2b. The calculated electric field, to be compared to Fig. 2a.

The  $S_{11}$  parameter of a simple rectangular patch of dimensions similar to those of structure in Figure 1 was compared to the  $S_{11}$  parameter of the combined structure to prove that joining a triangular and a rectangular patch increases the radiation area and provides a multi-resonating antenna. Comparison shown in Fig. 3 clearly establishes dual-band operation of the new structure.

## THEORETICAL STUDY OF MULTI-BAND MICROSTRIP ANTENNA

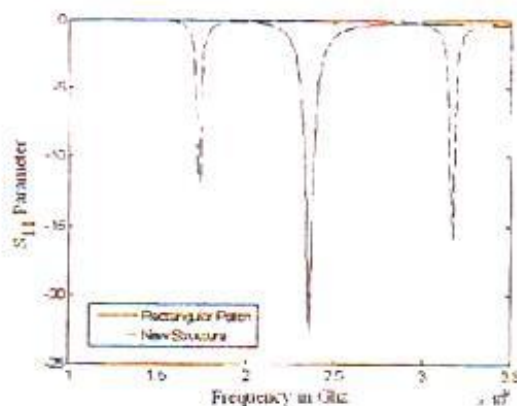


Figure 3 : The  $S_{11}$  parameter of a simple rectangular patch, and the  $S_{11}$  parameter of the structure shown in Fig. 1.

### FURTHER ANTENNA STRUCTURE AND RESULTS

The basic structure of the proposed antenna, shown in Figure 4, consists of three layers. The lower layer, which constitutes the ground plane, covers all the substrate and has a width of 6 cm and a length of 15 cm. The middle substrate, which is Polyflon Norclad, has a dielectric constant  $\epsilon_r = 2.55$  and a height of 0.32cm. The upper layer, which is the patch, consists of a rectangle with a width of 3 cm and a length of 4 cm, joined with an isosceles triangle having the same area as the rectangular patch and a base of 3 cm and a height  $h = 8$ cm. Inside the rectangular patch, ten rectangular slots, following a Chebyshev distribution around a central rectangular slot, were inserted. On the basis of parametric study and optimization carried out it was concluded that moving the feed deeper into the structure and putting it closer to the triangular slot made the functioning of the triangular slot more effective and gave the total response. The  $S_{11}$  parameter of the new antenna structure shown in Fig. 5 clearly exhibits GSM 900 MHz wide band operation in addition to operation at 2.8 GHz and 3.5 GHz.

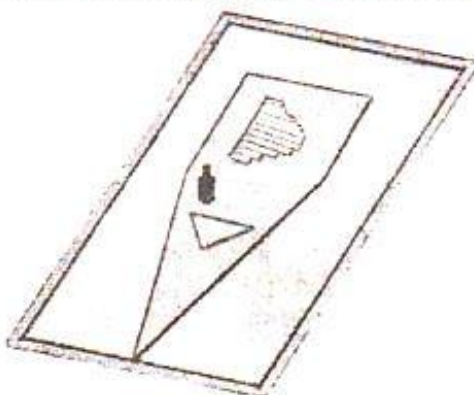


Figure 4 : The new antenna structure

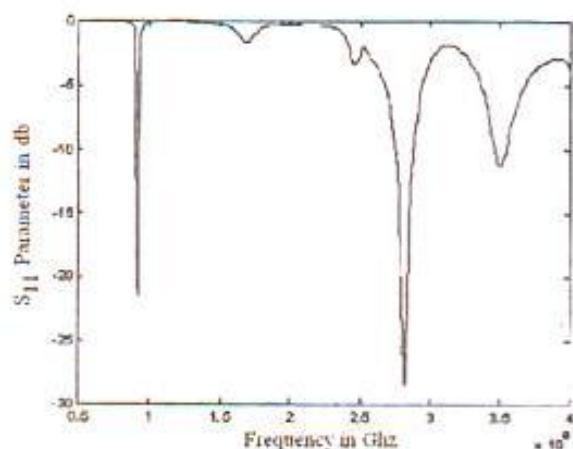


Figure 5 : The  $S_{11}$  parameter of the new antenna structure.

## CONCLUSION

A new multi-band antenna design has been presented. The design consists of joining a rectangular and a triangular patch together in one patch, and inserting several forms of slots. The new idea behind this design also includes the insertion of rectangular slots following a Chebyshev distribution around a central rectangular slot, in addition to a triangular slot inserted into the triangle, which has the same area as the rectangular patch. The concept of inserting slot arrays following a known antenna-array distribution has proven to give remarkable functionality to an antenna. It causes it to be highly radiating in different frequency ranges, using only one single feed, represented by a  $50\Omega$ .

The antenna has many applications, such as GSM, GPS, Wi-Fi, WiMax, video wireless communication, and Bluetooth applications, in one single instrument, using this type of antenna.

## REFERENCES

1. Balanis, C.A. *Antenna Theory Analysis and Design*, Second Edition, New York, Wiley, 1997.
2. Dong - Hee Park and Yoonsik Kwak.2007. "Design Multi-Band Microstrip Patch Antennas for Wireless Terminals" *Future generation communication and networking*, Volume. 1 : 439-441.

## THEORETICAL STUDY OF MULTI-BAND MICROSTRIP ANTENNA

3. Khairul, M., Ismail, H. and Esa, M.2003. "Low Profile Printed Antenna With A Pair of Step Loading for Dual-Frequency Operation," *Asia Pacific Conference On Applied Electromagnetics* (APACE 2003), Shah Alam, Malaysia, 2003.
4. Lee,K.F., Luk, K.M. and Dahele,J.S. 1988."Characteristics of the Equilateral Triangular Patch Antenna," *IEEE Transactions on Antennas and Propagation*, AP-36, 10, November 1988 : 1510-1518.
5. Ozlem, O., Selma, M., Aksun, M.I. and Alatan, L.2003. "Design of Dual-Frequency Probe Fed Microstrip Antennas with Genetic Algorithm," *IEEE Transactions on Antennas and Propagation*, AP-51, 8, August 2003 : 1947-1954.
6. Sittironnarit ,T. and Ali,M. 2002."Analysis and Design of a Dual-Band Folded Microstrip Patch Antenna for Handheld Device Application", *IEEE Southeast Conference Proceedings*, 2002 : 255-258.
7. Yang,F. and Rahmat-Samii,Y. 2003. "A Compact Dual Band Circularly Polarized Antenna Design For Mars Rover Mission," *IEEE International Symposium on Antennas and Propagation, Digest*, 3, June 22-27, 2003 : 858-861.

## ANALYSIS OF DIELECTRIC LENS ANTENNAS FOR MICROWAVE RADIATION DETECTOR

DHIRENDRA KUMAR, PRAKASH NAYAK\*

Department of Physics, Mithila Janta Inter College, Madhubani-847211 (Bihar)

\*P.G. Department of Physics, R.K. College, Madhubani-847211 (Bihar)

### ABSTRACT

We have analyzed an ideal microwave radiation detector using dielectric lens antennas. The dielectric lens consists of Electromagnetic Band Gap (EBG) super layers used to enhance the directivity of planer and wave guide antennas. We present and analyze the design and measurements of the beam pattern of the radiator.

**Key words :** Directivity, Waveguide, EBG, Microwave.

### INTRODUCTION

A great commercial interest exists in radio frequency identification devices, which are basically used to identify or track the objects. Other applications are access control, smart cards, logistics, etc. UHF and ISM can use both active and passive tag. Detailed information can be found in the bibliography [1, 2]. Typical successful read rates are nearly 80% to 95%, due to the attenuation caused by metallic and padding products [3, 4]. The numbers of elements that can be located in the focal plane of a dielectric lens is limited because the performance of the element located at a large distance from the central focus are significantly degraded with respect to the element in focus [5]. To increase the number of radiators on the ground plane, elements of larger directivity should be used so that they all excite efficiently the central portion of the lens is larger. This solution is effectively equivalent to increasing the F/D of the lens system.

### EBG Enhanced Dielectric Lenses

Modern research indicates that Electromagnetic Band Gap (EBG) super-layer can be used to enhance the directivity of planar and waveguide antennas as shown in figure 1.

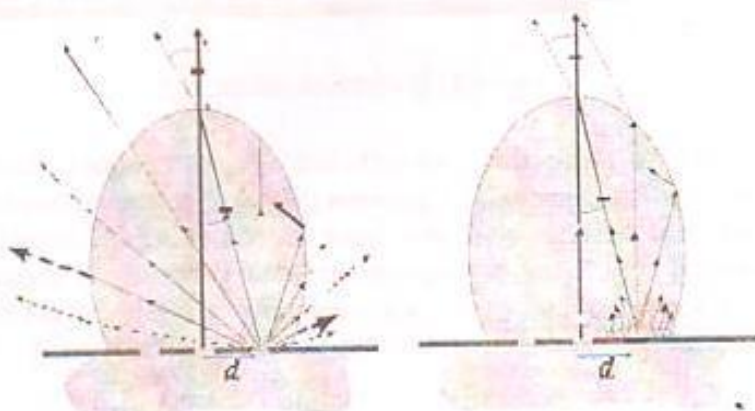


Figure 1 : Ray picture of an off focus fed dielectric lens, with and without leaky wave enhancement by means of EBG super-layer.

In [6, 7], the efficient excitation of reflector antennas by means of EBG enhanced printed waveguide feeds has been discussed. The main result is that the efficiency of single-feed reflectors and imaging arrays can be increased significantly with respect to radiators operating in free space, at low to moderate manufacturing cost. Here a similar design strategy has been applied to increase the efficiency of dielectric lens antennas. The use of EGB super-layers at microwave frequencies justified mainly by the electric performances of the systems, the manufacturing advantages of the EGB solutions based on dielectric may end up being the most important criteria in the microwave regimes. This particular difference can be understood from the intrinsic difficulty in realizing corrugated waveguide horns with micrometric accuracies and the integration of these horns with the receivers could be insurmountable.

#### Inverted Dielectric Stratification

The guidelines for a dielectric stratification to realize the optimal Fabry-Perot resonator also referred to as EBG structure, have been clarified to the antenna community by Jackson and Oliner [8], who provided a leaky-wave interpretation of the phenomenon.

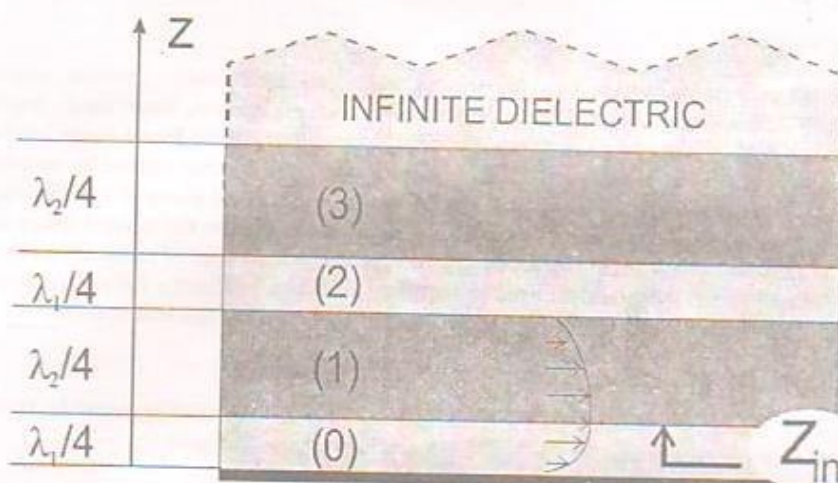


Figure 2 : Dielectric stratification

Two dominant (TE/TM) leaky waves are sufficient to represent main radiation in direction close to broadsides. If the upper layer is a dielectric lens antennas (Figure 2) instead of free space a series of quarter wavelength transformers will create an equivalent input impedance  $z_{in}$  that is very large instead of very small. In this way, a virtual open circuit or magnetic conductor is created. In Figure 2, layer (0) is than a quarter of the dielectric wavelength, shorted by a ground plane at  $z = 0$ . So, the field configuration of a waveguide with a lower electric wall and an upper magnetic wall is created.

## Analysis of dielectric lens antennas for Microwave radiation detectors

### Design of the Printed Radiators

The wave picture can be rigorously represented by identifying the two dominant poles in the Green's Function of the dielectric stratification. The directivity enhancement that can be achieved depends on the equivalent impedance contrast which is observed at  $Z_{in}$ . Given a fixed ratio between  $\epsilon_{r1}$  and  $\epsilon_{r2}$  such contrast can be enhanced to achieve higher directivities by using a large number of dielectric super-layers. However, such an increase of contrast leads to a smaller operating bandwidth.

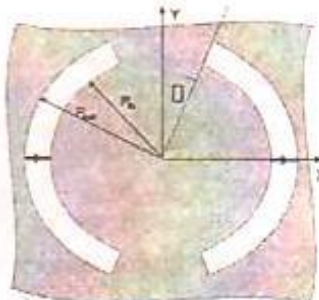


Figure 3 : Double slot configuration to achieve symmetric patterns

The trade-off between the bandwidth and the directivity guides in which only one layer of dielectric constant  $\epsilon_{r1} = 4$  (quartz) was applied to enhance this radiation in the lens of  $\epsilon_{r2} = 11.7$  (silicon). We decided to initially choose 10 GHz as design frequency [5]. Accordingly the lower slabs are 2.4 mm for the silicon layer and 3.75 mm for the quartz layer. A double slot radiator is designed, Figure 3. The central radius  $(R_{in}+R_{out})/2$  of this slot are set in such a way that an optimal excitation of the lens is achieved by minimizing the influence of higher order modes as in [6]. The width of the slots affects their impedance bandwidth while the length of each arc (defined by the angle  $\theta$ ) sets the central operating frequency. A nominal design with slabs tuned to 10 GHz operates well on a 10% bandwidth centered around 10.5 GHz for the following parameters,  $R_{in} = 2.6$  mm,  $R_{out} = 3.2$  mm and  $\theta = 22^\circ$ .

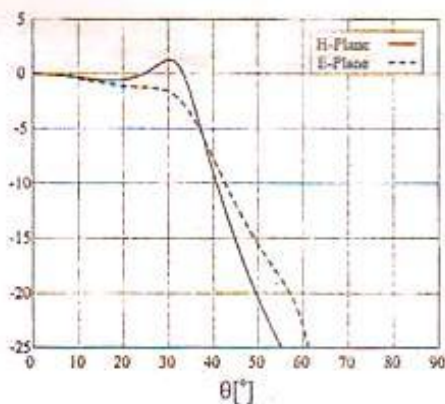


Figure 4 : Radiation Pattern

The radiation pattern of the double slot structure calculated at 10.5 GHz with software (HFSS) as shown in figure 4 exhibits almost perfect symmetry of the pattern as a function of the azimuth angle as well as the rapid drop off, which starts at about 30°. These properties ensure that the silicon dielectric lens excited by the twin slot will have high spill-over efficiency.

## CONCLUSION

We have successfully designed and measured the beam pattern of the microwave radiator with software H.F.S.S using Electromagnetic Band Gap (EBG) dielectric lens. We have been able to achieve a high spill – over efficiency by exciting silicon dielectric lens by twin slot.

## REFERENCES

1. K. Finkenzeller, *Fundamentals and Applications in contact less smart card and identifications*, New York, Wiley, 2003.
2. S. Garfinkel and B. Rosenberg, *RFIDs, Application, Security and Privacy*, Boston, MA, Addison-Wesley, 2005.
3. P. G. Ranky, *Assembly automation*, Vol. 26, no.1, pp 28-33, 2006.
4. D. Ciudad Rio-Perez, P Cobos Arribas, C. Aroca and P. Sanchez, *Testing Thick Magnetic Shielding Effects on a New Low Frequency RFIDs system*, *IEEE Trans on Antennas and Propag*, Vol. 56, no. 12, pp 3838-3843, Dec 2008.
5. Wu, X: Eleftheriades, G.V., van Deventer-Perkins, T.E.; *Design and Characterization of single and multiple-beam mm-wave circularly polarized substrate lens antennas for wireless communications* *Microwave theory and Techniques, IEEE Transactions on* Vol. 49, no. 3, pp 431-441, March 2001.
6. A. Neto, etal, *EBG Enhanced Feeds for High Aperture Efficiency Reflector Antennas*, *IEEE Trans. on Antennas and Propag.* Vol. 55 no. 08, Aug. 2007.
7. P. Day, etal., *A broadband superconducting detector suitable for use in large arrays*. *Nature* 425, 817-820, (2003)
8. D. R. Jackson, A. A. Oliner, *A Leaky-wave analysis of the high-gain printed antenna configuration*, *IEEE Trans. on Antennas and Propag.* Vol. 36, no. 7, pp. 905-909, July 1988.

## INTEGRATED E-SHAPE AND H-SHAPE BROADBAND MICROSTRIP PATCH ANTENNA

DHIRENDRA KUMAR

Department of Physics, Mithila Janta Inter College, Madhubani-847211 (Bihar)

AND

PRAKASH NAYAK

Head, P.G. Department of Physics, R.K. College, Madhubani-847211 (Bihar)

RECEIVED : 25 August, 2009

In this paper, proposed patch integrates both E- and H-shaped patch on same radiating element. The design adopts L-probe feeding, inverted patch and slotted patch techniques. The resonant properties of the proposed antenna have been predicted and optimized. Simulated result of the proposed antenna gives two closely excited resonant frequencies at 1.92 GHz and at 2.16 GHz. The simulated impedance bandwidth of 21% from 1.92 GHz to 2.16 GHz is achieved at 10 dB return loss.

### INTRODUCTION

The microstrip patch antenna is very well suited for applications such as wireless communications system, cellular phones, pagers, radar systems and satellite communications system [1, 2]. However, conventional microstrip patch antenna suffers from very narrow bandwidth. In recent years, researchers have offered several new microstrip patch configurations to increase the bandwidth of microstrip antenna. Well known methods to increase the bandwidth of antennas include increase of the substrate thickness, the use of low dielectric substrate, the use of various impedance matching and feeding techniques, the use of slot antenna geometry and the use of multiple resonators [3-6]. A novel single layer wide-band rectangular patch antenna with achievable impedance bandwidth of greater than 20% has been demonstrated [7]. Utilizing the shorting pins or shorting walls on the unequal arms of a U-Shaped patch, U-slot patch or L-Probe feed patch antennas, wideband and dual band impedance bandwidth have been achieved with electrically small size in [8, 9]. Other techniques involves employing multilayer structures with parasitic patches of various geometries such as E, V and H shapes, which excites multiple resonant modes but all generally fabricated on thicker substrate [10].

In this paper, investigation is made for enhancing the impedance bandwidth on a thin substrate (about  $0.01\lambda_0$ ) using novel slotted shape patch. To meet design requirement the L-probe feeding inverted patch and slotted patch techniques have been employed. Design and simulation results of the novel wideband microstrip patch antenna is presented.

### PROPOSED ANTENNA DESIGN

The geometry of the proposed patch antenna is shown in figure 1. The inverted rectangular patch of width  $W$  and length  $L$  is supported by a low dielectric superstrate with dielectric permittivity  $\epsilon_r$  thickness  $h_1$ .

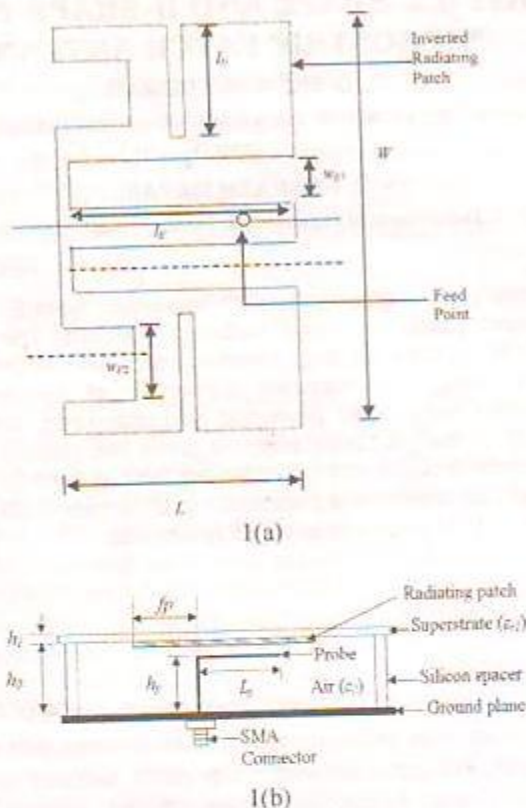


Fig. 1. Proposed patch antenna (a) Top view and (b) Side view

An air-filled substrate with dielectric permittivity  $\epsilon_0$  and thickness  $h_0$  is sandwiched between the superstrate and a ground plane. The proposed patch integrates both  $E$ - and  $H$ -shaped patch on the same radiating element. For the  $E$ -shaped, the slots are embedded in parallel on the radiating edge of the patch symmetrically with respect to the centerline (x-axis) of the patch and for the  $H$ -shaped the slots are embedded in serial on the non-radiating edge of the patch. The  $E$ - and  $H$ -shaped are shown in figure 1(a), where  $l$  and  $w$  are the length and width of the slots. The patch is fed by an  $L$ -shaped probe with height  $h_p$  and horizontal length  $l_p$  along the  $x$ -axis at a distance  $f_p$  from the edge of the patch as shown in figure. 1(b). The optimized design parameters obtained for the proposed antenna is shown in Table 1.

Table 1 : Patch antenna parameter.

Parameters	Value (mm)
$h_1$	1.4827
$h_0$	16.1
$W$	78.0
$L$	37.0
$l_H$	17.0
$ El $	36.00
$w_{E1}$	3.8
$w_{E2}$	10
$f_p$	6.5
$h_p$	12.5
$l_p$	24.5

The use of *L*-probe feeding technique with a thick air filled substrate provides the bandwidth enhancement, while the application of superstrate with inverted radiating patch offers gain enhancement. The use of parallel and series slots reduce the size of the patch. By incorporating extra slots in radiating edge, improvement in gain and cross polarization has been achieved.

## SIMULATION RESULTS

**S**imulation result of the return loss of the proposed antenna is shown in figure 2. The resonant properties of the proposed antenna have been predicted and optimized using HFSS. The two closely excited resonant frequencies at 1.92GHz and at 2.16GHz as shown in figure 2 gives the measure of the wideband characteristics of the patch antenna. The simulated impedance bandwidth of 21% from 1.92 GHz to 2.16GHz is achieved at 10 dB return loss.

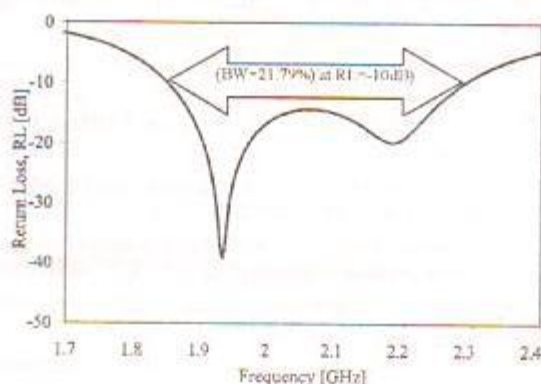


Fig. 2 : Simulated return loss.

Figure 3 shows the radiation pattern of proposed patch antenna at the second resonant frequency for *xz*-plane and *yz*-plane. The designed antenna displays good broadside radiation pattern at upper resonant frequency. The *L*-probe inverted proposed patch antenna exhibits better cross polarization and the radiation characteristics compared to conventional patch antenna.

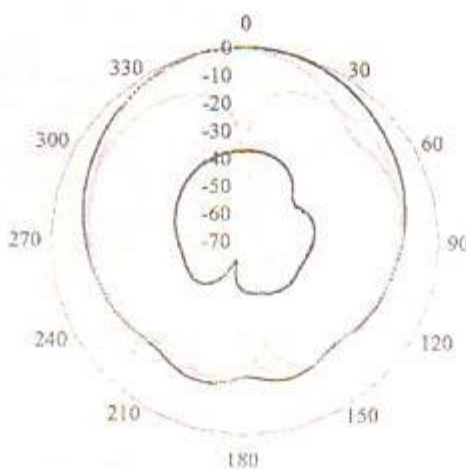


Fig. 3 : Radiation pattern of proposed patch antenna.

## CONCLUSION

In this paper a novel technique for enhancing bandwidth of microstrip patch antenna has been successfully achieved. Techniques for microstrip broadbanding, size reduction and cross polarization reduction are applied with significant improvement in the design by employing proposed slotted patch shape design, inverted patch and *L*-probe feeding.

The proposed microstrip patch antenna achieves a fractional bandwidth of 21% (1.92 to 2.16 GHz) at 10dB return loss.

## REFERENCES

1. Stutzman, W.L. and Thiele, G.A., *Antenna Theory and Design*, 2<sup>nd</sup> ed, New York, Wiley (1998).
2. Balanis, C.A., *Antenna theory*, 2<sup>nd</sup> ed., New York, John Wiley & Sons, Inc. (1997).
3. Kumar, G. and Ray, K.P., *Broadband microstrip antenna*, Artech House Inc. (2003).
4. Wi, S.H., et al., Package-Level integrated antennas based on LTCC technology. *IEEE Trans. on Antennas and Propag.* 54(8), 2190-2197, (2006).
5. Wi, S.H., et al., Bow-tieshaped meander slot antenna for 5 GHz application. in *Proc. IEEE Int. Symp. Antenna and Propagation*. 2, 456-459, (2002).
6. Matin, M. M., et al., Probe fed stacked patch antenna for wideband applications. *IEEE Trans. on Antennas and Propag.* 55(8), 2385-2388, (2007).
7. Yang, F., Zhang, X., Rahmat-Samii, Y. Wide-band E-shaped patch antennas for wireless communications, *IEEE Trans. on Antennas and Propag.* 49(7), 1094-1100, (2001).
8. Guo, Y.X., et al., A quarter-wave U-shaped antenna with two unequal arms for wideband and dual-frequency operation. *IEEE Trans. on Antennas and Propag.* 50, 1082-1087, (2002).
9. Chair, R., et al., Miniature wide-band half U-slot and half E-shaped patch antennas. *IEEE Trans. on Antennas and Propag.* 53, 2645-2652 (2005).
10. Bao, X.L., Ammann, M.J., Small patch/slot antenna with 53% input impedance bandwidth. *Electronics Letters*. 43(3), 146-147 (2007).

□

## Effect of substrate height on compact broadband microstrip patch antenna

Dhirendra Kumar

Department of Physics,  
Mithila Janta Inter College,  
Laheriaganj, Madhubani-847211, Bihar, (India)  
and  
Prakash Nayak

Head, P. G. Department of Physics,  
R. K. College, Madhubani-847211, Bihar, (India)

(Received for publication in August, 2009)

[ Abstract : In recent years, the major fraction of research on microstrip and printed antenna is devoted to develop new design to improve antenna bandwidth along with other figures of merit. In this paper, a new dual frequency antenna is described. Freedom for tuning the resonant frequencies is available because of more design parameters. The theoretical analysis is based on the finite difference time domain (*FDTD*) method. The effects of relative permittivity of substrate and substrate height on two resonant frequencies are presented and discussed. ]

### Introduction

With the development of *MIC* and high frequency semiconductor devices, microstrip has drawn maximum attention of the antenna community in recent years. In spite of it, various attractive features like, light weight, low cost, easy fabrication, conformability on curved surface, the microstrip element suffers from an inherent limitation of narrow impedance bandwidth. So, along with other development, widening the bandwidth of microstrip elements has become a major branch of activities in the field of printed antenna. Many books<sup>1-3</sup> and many chapters<sup>4-6</sup> have covered the development occurred time to time during the last two decades. The dual frequency microstrip antenna with a single feed are required in radar and communication system, such as Synthetic Aperture Radar (*SAR*), dual band *GSM/DCS* mobile communication and the *GPS*. Dual frequency operation of microstrip antenna with a spur-line filter embedded in the patch has also been reported<sup>7</sup>. It shows a frequency ratio of  $\sim 2.0$  between the two operating frequencies. In dual frequency, the lower and higher operating frequencies are designed at the resonant frequencies of a new resonant mode, generated by the perturbation of

the embedded spur-line filter in the patch, and the transverse magnitude ( $TM_{01}$ ) mode. Dual slot-loaded microstrip antenna with dual frequency have been presented<sup>8-9</sup>, where two parallel narrow slots are etched in the rectangular patch close to its radiating edges. In this paper, a novel compact dual frequency antenna is proposed and studied for effect of substrate height.

#### Antenna model

The configuration of the novel compact dual frequency antenna is shown in figure 1. The antenna consists of an *H*-shaped microstrip patch, supported on a grounded dielectric sheet of thickness  $h$  and dielectric constant  $\epsilon_r$ . The patch has a total length of  $a$  and a width of  $b$ . The three distinct parts of the patch comprises : a centre conductor strip with length  $d$  and width  $s$  and two identical conductors strips with length  $w$  and width  $b$  on both sides. A shorting pin with a radius of  $r_s$  is loaded at the centre line of the *H* shaped patch, with a distance of  $d_s$  from the radiating edge and the feed point is located at the centre line of the *H*-shaped patch with a distance of the  $d_f$  from the radiating edge.

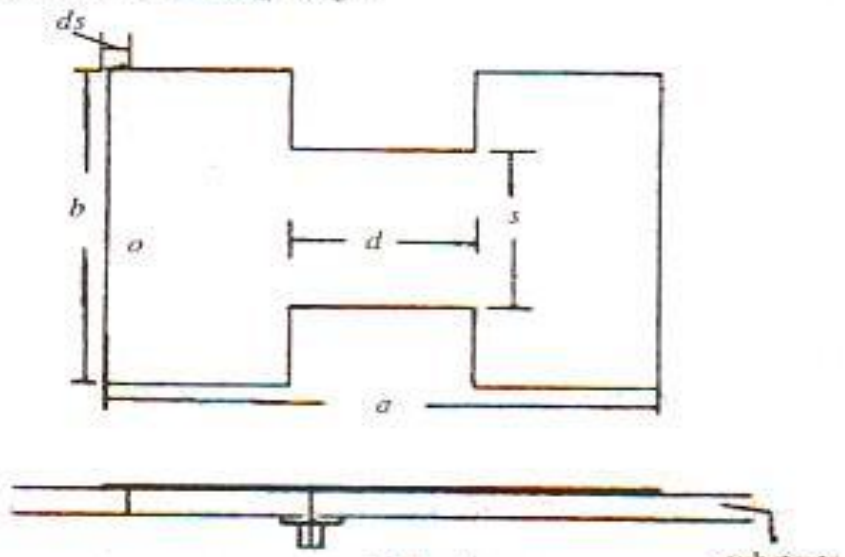


Fig. 1  
Proposed dual-frequency antenna.

#### Numerical analysis

For numerical analysis of this antenna, we have used the *FDTD* algorithm which is used to analyze antennas of complex structures.

A Gaussian pulse voltage with unit amplitude is given by

$$V(t) = \exp [-(t - t_0)^2/T^2], \quad \dots \quad (1)$$

where  $T$  denotes the period and  $t_0$  identifies the centre time is excited in the probe feed. For the feed probe, we use a series resistor  $R_s$  with the voltage generator to model the current in the feed probe. The input impedance of the antenna is obtained from

$$Z_{in} = \frac{V(f)}{I(f)} - R_s. \quad \dots \quad (2)$$

The result of input impedance are then used to obtain the return loss characteristics of the antenna. To find the radiation pattern characteristics, a sinusoidal excitation at probe feed is used which is given by

$$V(t) = \sin(2\pi f_0 t). \quad \dots \quad (3)$$

where  $f_0$  denotes the resonant frequency of interest. The field distributions are recorded at one instant of time after the steady state has been reached. In our analysis, the total time for stability is more than six cycles. After the field distribution has been obtained, the radiation pattern can be calculated by using the near field to far field transformation.

#### *Effect of relative permittivity of substrate*

The two resonant frequencies of  $f_{01}$  and  $f_{03}$  with different value of  $\epsilon_r$  are presented in figure 2. It is shown that with the increase of  $\epsilon_r$ ,

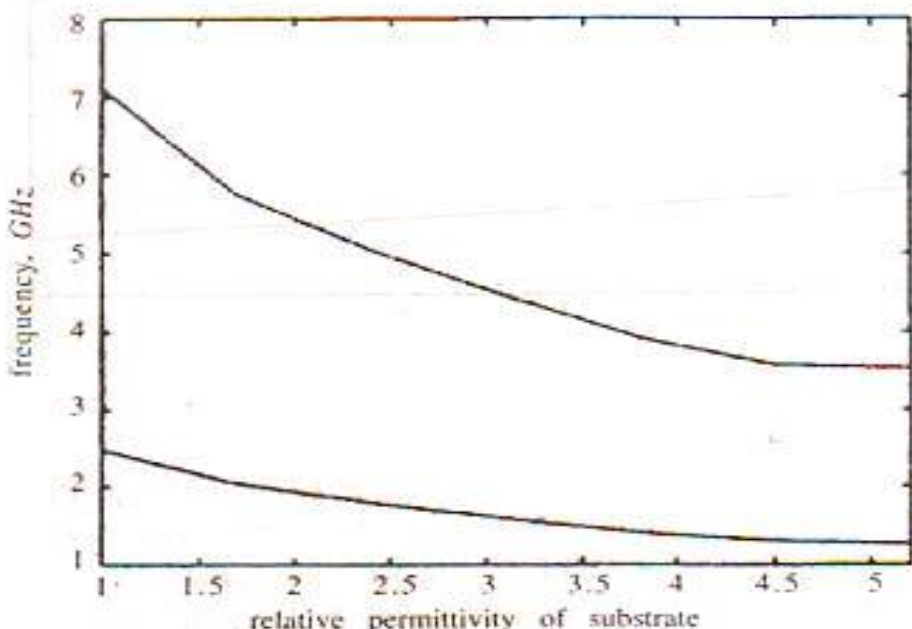


Fig. 2  
Resonant frequency with  $\epsilon_r$ .

the resonant frequencies at both  $TM_{01}$  and  $TM_{03}$  modes decreases. When the value of  $\epsilon_r$  equals 1.0, the frequencies  $f_{01}$  and  $f_{03}$  reach the maximum value 2.47 and 7.11 GHz. The  $f_{01}$  and  $f_{03}$  reach the value of 1.27 and 3.53 GHz, when the value of  $\epsilon_r$  is increased to 5.2. In this calculation, other parameters of the shorting pin - loaded *H*-shape patch are fixed as  $a = 20$  mm,  $b = 20$  mm,  $s = 4$  mm,  $d = 10$  mm,  $r_s = 0.4$  mm,  $d_s = 1$  mm and  $h = 1.6$  mm. The frequency ratio shows a slow decrease from 2.88 to 2.78 with a value of  $\epsilon_r$  changing from 1.0 to 5.2.

#### *Effect of substrate height*

The two resonant frequencies of  $f_{01}$  and  $f_{03}$  with different values of substrate thickness  $h$  are presented in figure 3.

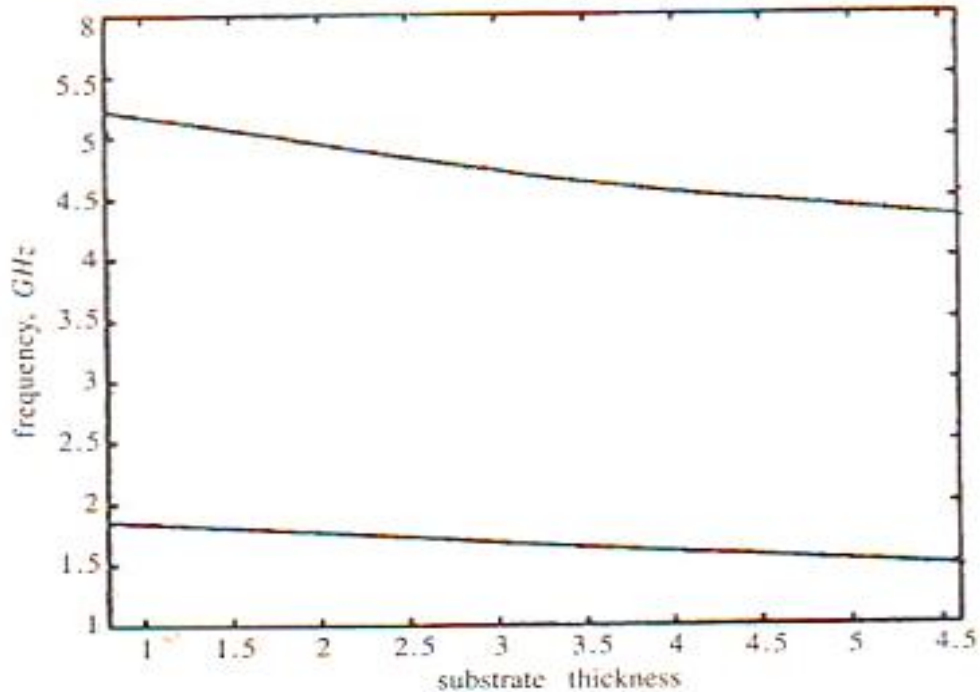


Fig. 3  
Resonant frequency with  $h$ .

It is shown that with the increase of  $h$ , the resonant frequencies at both the  $TM_{01}$  and  $TM_{03}$  modes decreases. When the value of  $h$  equal 0.8 mm, the frequencies  $f_{01}$  and  $f_{03}$  reaches the values of 1.85 and 5.22 GHz. When the value of  $h$  increases to 5.6 mm, the frequencies  $f_{01}$  and  $f_{03}$  reach the value of 1.49 and 4.35 GHz. In this calculation, other parameters of the shorting - pin - loaded, *H*-shaped patch are

fixed at  $a = 20 \text{ mm}$ ,  $b = 20 \text{ mm}$ ,  $d = 10 \text{ mm}$ ,  $s = 4 \text{ mm}$ ,  $r_s = 0.4 \text{ mm}$ ,  $d_s = 1 \text{ mm}$  and  $\epsilon_r = 2.33$ . The frequency ratio shows of slight increase from 2.82 to 2.915 with the value of  $h$  changing from 0.8 mm to 5.6 mm.

### Conclusion

A new compact, dual frequency microstrip antenna is presented in this paper. To achieve compact size, this antenna takes advantage of the compactness of *H*-shaped patch antenna and the dual frequency operation provided by a shorting pin. The variation of two resonant frequencies with respect to substrate permittivity ( $\epsilon_r$ ) and substrate thickness ( $h$ ) are illustrated and discussed. It is shown that this dual frequency antenna is very compact in size and can obtain a wide range of variation in frequency. Research work is currently on to investigate methods for broadening antenna bandwidth.

### References

1. Zurcher, J. F. and Gardiol, F. E.—Broadband microstrip antennas, Artech House, Boston.
2. Kumar, Girish and Ray, K. P.—Broadband patch antennas, Artech House, Boston.
3. Wong, W. L.—Compact and broadband microstrip antennas, Wiley, N.Y., (2002).
4. Griffiths, L. A. et. al.—Broadband and Multiband Antenna Design using the Genetic Algorithm to create Amorphous shapes using Ellipses, IEEE Trans. Antenna Propag., Vol. 54, No. 10, pp. 2778-2782, Oct. (2006).
5. Garg, R. et. al.—Ch. 9 in Microstrip Antenna Design Handbook, Artech House, Boston.
6. Guo, Y. -X. ; Khoo, K. -W. and Ong, L. C.—Wideband dual polarized patch antennas with Broadband Baluns, IEEE Trans. antenna Propag., Vol. 55, No. 1, pp. 78-83, Jan. (2007).
7. Serrano-Vaello, A. and Sanchez-Hernandez, D.—Printed antennas for dual-band GSM/DCS 1800 mobile handsets, Electron. Lett., 34(2), 140-141, (1998).
8. Maci, S. ; Biffi Gentili, G. ; Piazzesi, P. and Salvador, C.—Dual-band slot-loaded patch antenna, IEEE Proc. Part H Microwaves Antenna Propag., 142, 225-232, (1995).
9. Aeimovic, I. ; Namara, D. A. and Petosa, A.—Dual Polarized Microstrip Patch Planar Array Antenna with Improved port - to - port Isolation, IEEE, Trans. Antennas Propag., Vol. 56, No. 11, pp. 3433-3439, Nov. (2008).

## Study of effect of shorting wall length for designing a compact circularly polarised microstrip patch antenna

Prakash Nayak

Principal investigator, UGC-MRP,

Head, P.G. Department of Physics,

R.K. College, Madhubani-847211, Bihar, India

E-mail : prakashnayak.17@gmail.com

and

Dhirendra Kumar

Project Fellow, UGC-MRP, P.G. Department of Physics,

R.K. College, Madhubani-847211, Bihar, India

E-mail : k.dhirendra17@gmail.com

(Received for publication in July, 2011)

**[Abstract :** In this paper, an antenna design showing good circularly polarised with a reduction in its size by 25% from conventional rectangular patch antenna is presented. The effect of variation of shorting wall length with patch size to achieve desired resonance frequency and with truncated length for optimum axial ratio were examined. The measured data for the fabricated antenna is taken by *ES* vector network analyser. The theoretical analysis is based on the High Frequency Software Simulator. The designed antenna finds application at civilian *GPS* frequency (1.498 GHz).]

### Introduction

Now-a-days patch antenna with high permittivity sintered material substrate are used for *GPS* applications. These very compact automotive antenna are quite expensive and enough prone to circular polarization degradation due to the positioning of the antenna on the car body, as a rule near the scattering edge of the metallic roof<sup>1</sup>. Many application in communication and radars requires circular or dual linear polarization and the flexibility afforded by microstrip antenna technology has led to a wide range of designs and techniques to fill this need<sup>2-3</sup>. The demand for compact mobile telephone handsets has grown. Handsets with size of a pocket have begun appearing in the market and as the demand for increased electronic mobility grows, the need for small handsets will mostly increase. A small antenna is required for these handsets. The reduction of the patch size can be achieved by using patch substrate materials with very high permittivity and small substrate height<sup>4</sup>. It is demonstrated that the

bandwidth of circular polarised can be significantly increased when one more parasitic loop is added inside the original loop<sup>5</sup>. Novel applications of Global positioning system technology requires innovations such as time dependent, real time and near real time positioning at data acquisition times of only a few seconds. This fast observation rate enables the analysis of many dynamic phenomena that often encountered in Earth and atmosphere science. F. Scirè scappuzzo and S.N. Makarov<sup>6</sup> compared the performance of the classic *GPS* choke ring ground plane with a new shallower design. In this case, the low radiation efficiency will reduce the antenna gain. Various techniques have been explored to develop small size antenna. One of these techniques is achieved by using shorting wall<sup>7</sup>.

The objective of this paper is to study the effect of the shorting wall length on the polarization of the shorted Rectangular Microstrip Patch Antenna and to design a compact circularly polarised *MPA* which operates at the civilian resonance frequency (1.498 GHz) for the Global Positioning system.

#### *Antenna configuration and simulated results*

The *SRMPA* geometry is shown in figure 1. The feed point is centered on the *x*-axis and the shorting wall is at the patch edge.

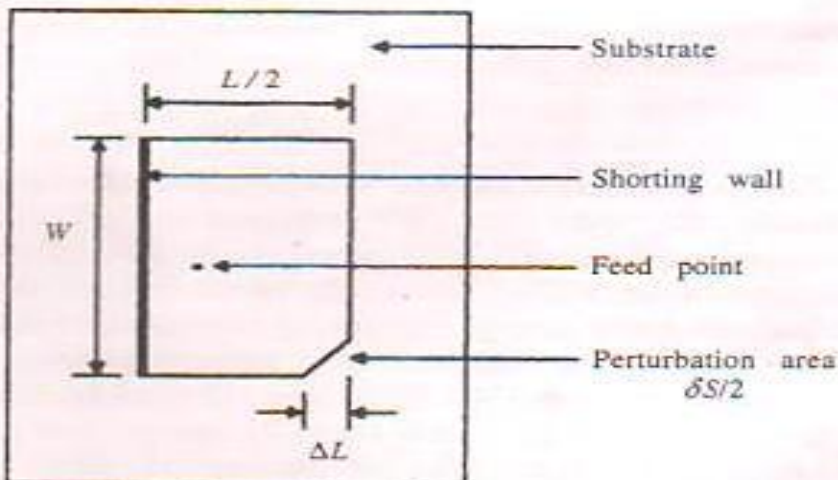


Fig. 1  
Configuration of circularly polarized *SRMPA*.

The antenna is circularly polarized *CP* by the single feed technique with a truncated segment setting to the edge of the patch

with equal side length  $\Delta L$  and area of  $\delta S/2$ . The SRMPA has a side length  $L/2$  and width  $W^*$ . The input impedance and resonance frequency of the SRMPA can be controlled by changing the length of the shorting wall<sup>9</sup>. To study the effects of shorting wall length on the SRMPA parameters, a proposed antenna is specified as in table 1 and simulated with HFSS software with different shorting wall lengths.

**Table 1**  
*Proposed antenna specification.*

$f_r$	$\epsilon_r$	$h$	$W$	$L/2$	$\Delta L$
1.498 GHz	2.1	1.48 mm	62.32 mm	36.74 mm	4.2 mm

The simulated results show that when the shorting wall length is reduced, the resonance frequency is decreased. To have the same resonance frequency, the patch lengths ( $L/2$ ,  $W$ ) have to be reduced resulting in patch size reduction. Due to the reduction in the patch size, the patch axial ratio (AR) will be degraded. To improve the AR, the perturbation segment length  $\Delta L$  must be readjusted.

**Table 2**  
*Variation of SW with  $f_r$  and AR.*

New SW length (mm) (% of SW = 62.32 mm)	New frequency (GHz) (% of $f_r = 1.498$ GHz)	New $\Delta L$ (mm) for best AR	Axial ratio for	
			Old $\Delta L$	New $\Delta L$
52.36 (84.0%)	1.494 (99.7%)	4.1	6.64	1.12
51.27 (82.3%)	1.491 (99.5%)	3.9	6.21	1.10
50.18 (80.5%)	1.489 (99.4%)	3.6	5.94	1.02
49.65 (79.7%)	1.484 (99.1%)	3.2	6.65	1.01
47.32 (75.9%)	1.474 (98.4%)	2.5	6.26	1.09
42.47 (68.1%)	1.404 (93.7%)	2.4	5.01	1.06
34.56 (55.5%)	1.336 (89.2%)	2.3	6.36	1.01
27.22 (43.7%)	1.221 (81.5%)	2.1	6.28	1.00

Table 2 illustrates the relation between shorting wall length (SW), new resonance frequency, new truncated length  $\Delta L$  to have the best AR at bore-sight (angle  $\theta = 0$ ), and axial ratio for old and new  $\Delta L$ .

Figure 2 shows the variation of the shorting wall length ( $SW$ ) with patch size to have the desired resonance frequency  $f_r = 1.498$ , while figure 3 shows the variation of the shorting wall length ( $SW$ ) with the truncated length ( $\Delta L$ ) for optimum axial ratio.

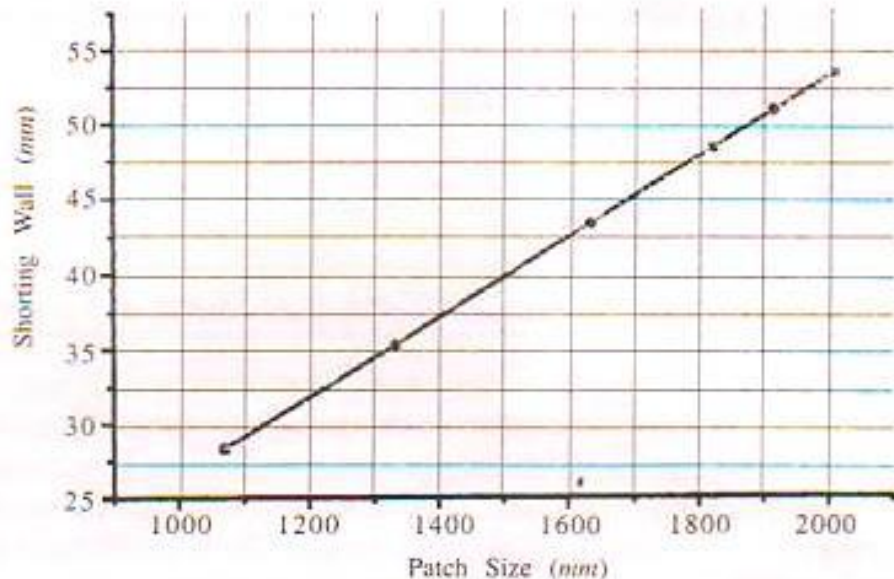


Fig. 2  
Variation of shorting wall length with patch size.

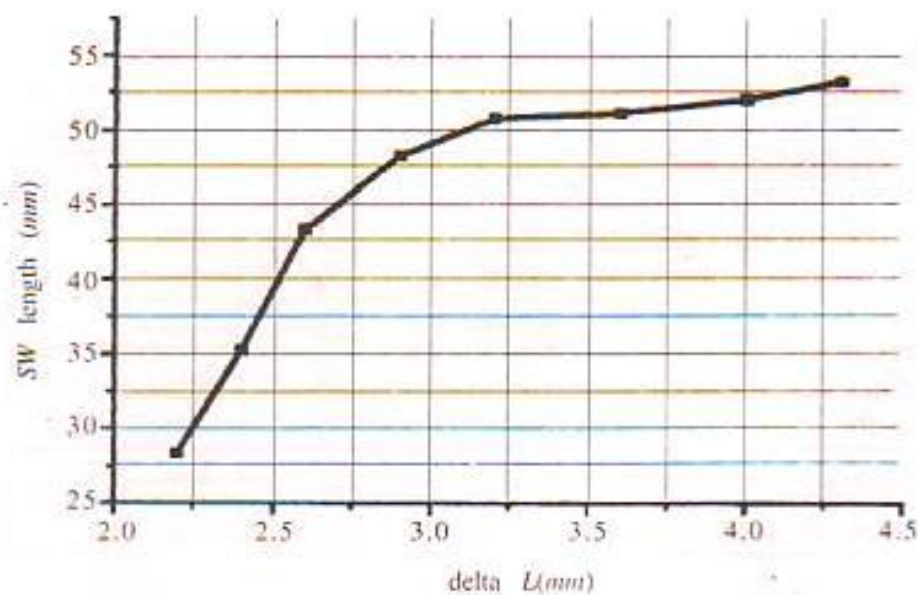


Fig. 3  
Variation of shorting wall length with truncated length.

*Compact circularly polarized partially SRMPA*

As a result of the previous study, the design of a right hand circularly polarized (*RHCP*) partially *SRMPA* operating at the civilian resonance frequency of the Global Positioning System is considered. The antenna configuration is shown in figure 1 and antenna parameters calculated from *HFSS* are given in table 3.

**Table 3**

*Specifications of the RHCP partially SRMPA.*

$f_r$	$\epsilon_r$	$h$	$W$	$L/2$	$\Delta L$	$SW$
1.498 GHz	2.1	1.48 mm	39.39 mm	28.05 mm	2.10 mm	27.32 mm

Scattering parameters and input impedance are measured using *ES* network analyser. Simulated results of the *RHCP* partially *SRMPA* for the *GPS* are given in table 4.

**Table 4**

*Simulated results of the RHCP partially SRMPA.*

Parameters	Partially SRMPA
Beam width	71°
Directivity	2.68 dBi
Axial ratio	1.00
Return loss	-26.12

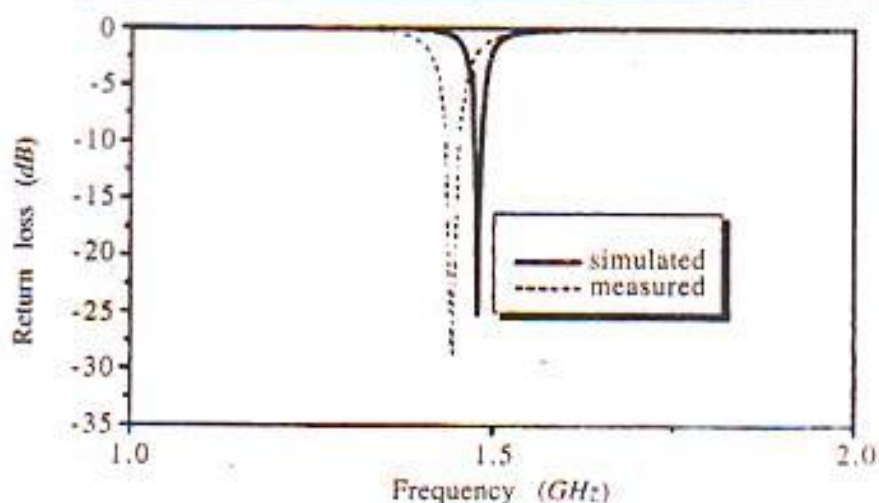


Fig. 4

Comparison between simulated and measured return loss of the *RHCP* partially *SRMPA*.

### Conclusion

The effect of variation of shorting wall length with patch size to achieve desired resonance frequency and with truncated length for optimum axial ratio were examined. Simulations and measurements on the partially shorted rectangular microstrip patch antenna have provided a useful design for a compact circularly polarised antenna operating at civilian resonance frequency of 1.498 GHz for GPS applications. Also, 25% reduction in antenna size from conventional antenna is achieved.

### References

1. Chen Wen-Shyang, chun-kunwn Wong Kin-Lu—Novel compact circularly polarized square microstrip antenna, *IEEE Transaction on Antennas and Propagation*, 49(3), pp. 340-342 (2001).
2. Wong Kin-Lu—Compact and Broadband Microstrip Antennas, (John Wiley and Sons, Inc.) (2002).
3. Kumar, D. ; Nayak, P. and Jha, L.—Theoretical study of Multi-Band Microstrip Antenna, *Bulletin of Pure and Applied Sciences*, 28 D(1), pp. 1-7 (2009).
4. James, J. R. ; Hall, P. S. and Wood, C.—Microstrip Antenna Theory and Design, (Peter Perigrinus, London). (1981).
5. Li-R, De Jean G. ; Laskar, J. and Tentzeris, M. M.—Investigation of circularly polarized loop antennas with a parasitic element for band width enhancement, *IEEE Transaction on Antennas and Propagation*, 53 (12), pp. 3930-3939 (2005).
6. Scappuzzo-F, Scire' and Makarov, S. N.—A low multipath wideband GPS antenna with cut-off or non-cut-off corrugated ground plane, *IEEE Transaction on Antennas and Propagation*, 53(1), pp. 33-46 (2009).
7. Sanad, M.—A small size microstrip antenna having a partial short Circuit, *IEEE International Conference on Antenna and Propagation*, 1, pp. 465-471 (1995).
8. James, J. R. and Hall, P. S.—Handbook of microstrip antennas, (Peter Perigrinus Ltd., London) (1989).
9. Taga, T. and Tsuna Kawa K.—Performance analysis of a built-planar inverted-F antenna for 800 MHz band portable radio Units, *IEEE Journal on selected areas in communication*, 5(5), pp. 921-929 (1987).

shows the simulated radiation pattern of the *RHCP* partially *SRMPA* at 1.498 GHz. Figure 6 shows the simulated axial ratio results of the *RHCP* partially *SRMPA*. The measured and simulated results are accepted and satisfy the requirements for a *GPS*.

## TRANSFORMING MAXWELL'S EQUATION INTO EQUIVALENT SCHRODINGER EQUATION FOR THE PHOTONIC BAND GAP STRUCTURE

DR. PRAKASH NAYAK

*Principal Investigator, Reader and Head, P.G. Deptt. of Physics, R. K. College, Madhubani (Bihar), India*  
AND

DR. DHIRENDRA KUMAR

*Project Fellow, UGC-MRP, P. G. Deptt. of Physics, R. K. College, Madhubani (Bihar), India*

RECEIVED : 13 December, 2011

In analogy with Kronig-Penney model for electronic band-gaps in periodic potentials, Maxwell's equation for the propagation of light in the photonic crystal are transformed into an equivalent form of Schrodinger's equation. In the THz frequency range, the propagation of electromagnetic waves through doped semiconductors such as silicon is well represented by a frequency dependent Drude model.

### INTRODUCTION

Photonic Band Gap (PBG) structures are periodic structures in which optical waves are forbidden in certain frequency bands. The PBG problem is a matter of solving the macroscopic Maxwell's equation for wave propagation in periodic media. Periodic changes in potential impose periodic boundary conditions on propagating EM modes. Electromagnetic waves not matched to those boundary conditions can not propagate.

Treatments of photonic crystals typically draw an analogy between the solution to Schrodinger's equation for a periodic potential which leads to solid-state band gap structures and the solution of Maxwell's equation with a periodic dielectric constants, which leads to photonic band gap structures [1, 2, 14, 15]. However, the mathematical analogy between electron band gaps and photonic band gaps is limited [3]. Analytical solutions for photonic band-gap crystals are rare, one of the reasons being Maxwell's equations for photonic band-gap crystals have the additional constraint that EM waves are transverse, whereas the wave function of Schrodinger's equation does not have this limitation.

In this paper alternate layers of doped and un-doped silicon sheets as the photonic band gap materials have been utilized in our models. The alternating layers form a one-dimensional lattice that forms a periodic potential energy in the propagation direction, normal to the silicon layers. Attempt has been made to transform Maxwell's equation into a form equivalent to Schrodinger's equation for a one dimensional periodic square well potential energy in a crystal and Kronig-Penney type solutions [4, 5, 6] were worked out to calculate photonic band-gap structure.

#### Transformation of Maxwell's Equation :

Maxwell's equations in CGS unit are

$$\nabla \times E = -\frac{1}{c} \frac{\partial B}{\partial t} \quad \dots (1)$$

$$\nabla \times B = \frac{1}{c} \epsilon_{\infty} \frac{\partial E}{\partial t} + \frac{4\pi J(z)}{c} \quad \dots (2)$$

where  $\epsilon_{\infty}$  is the contribution to the dielectric constant due to bound charges, which does not depend on the dopant density.  $J(z)$  is the periodic current density induced by free charges.

The time independent Schrodinger's equation is written as

$$-\frac{\hbar^2}{2m} \frac{\partial^2 \psi}{\partial z^2} + U(z) \psi = \epsilon \psi \quad \dots (3)$$

where  $\psi$  is the eigenfunction and  $\epsilon$  is the energy eigenvalue of the particle with mass  $m$  moving in a square well periodic potential  $U(z)$  shown in fig. 1.

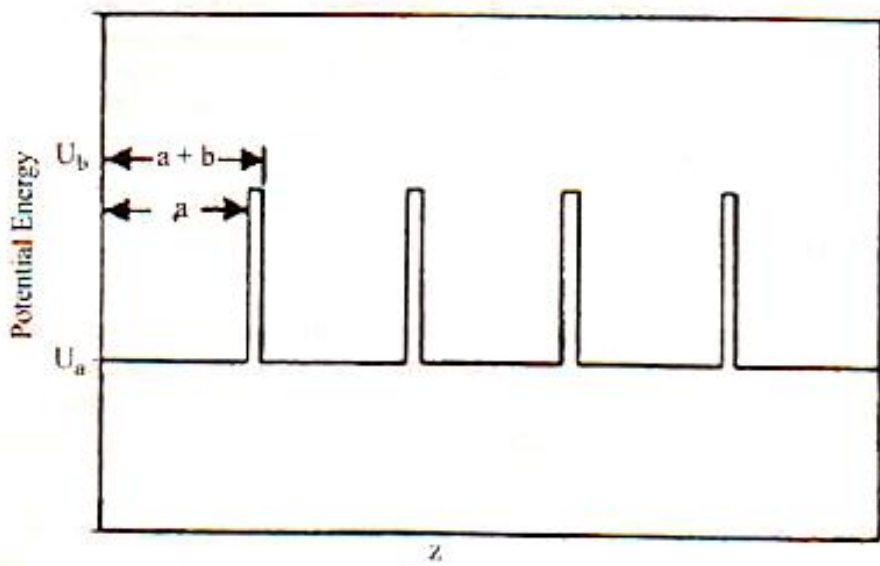


Fig. 1

Dividing through by  $\frac{\hbar^2}{2m}$  we obtain

$$-\frac{\partial^2 \psi}{\partial z^2} + \frac{2mU(z)}{\hbar^2} \psi = \frac{2m\epsilon}{\hbar^2} \psi \quad \dots (4)$$

The potential of the un-doped silicon,  $U_a$ , is assumed to be negligible compared to the potential of the doped silicon,  $U_b$ . The condition for traveling wave solution,  $\psi = a \exp(-ikz)$ , through a square well periodic potential of finite width  $b$  and lattice spacing  $a + b$  is [5].

$$\cos k(a+b) = \frac{Q^2 - k^2}{2QK} \sin h(Qb) \sin(ka) + \sin(Qb) \cos(ka) + \cos h(Qb) \cos(ka) \quad \dots (5)$$

$$K = \sqrt{\frac{2m\epsilon}{\hbar^2}} \quad \dots (6)$$

and

$$Q = \sqrt{\frac{2mU_b}{h^2} - \frac{2m\epsilon}{h^2}} \quad \dots (7)$$

In the limit of delta function periodic potential barriers where  $b \rightarrow 0$  and  $U_b \rightarrow \infty$ , the condition for travelling wave solution is

$$\cos(Ka) = \frac{P}{Ka} \sin(Ka) + \cos(Ka) \quad \dots (8)$$

where

$$P = \frac{Q^2 ba}{2} \quad \dots (9)$$

Most approaches that relate the Kroning-Penney model with photonic band-gap materials are directed toward solving equation (4) for which dielectric constant varies periodically in space and is purely real (that is, there are only travelling wave solution) and  $J(Z) = 0$ . Moreover these approaches assume that the dielectric constants, or equivalently the index of refraction is independent of frequency [7, 8, 11, 12]. Clearly this assumption is not valid when the frequency of electromagnetic is comparable to the plasma frequency of the doped regions.

In the present case, it is the free charges that are periodic. If we substitute eqn. (2) into the curl of eqn. (1), we obtain

$$\nabla^2 \mathbf{E} = -\frac{1}{c^2} \epsilon_{\infty} \frac{\partial^2 E}{\partial t^2} - \frac{4\pi}{c^2} \frac{\partial J(Z)}{\partial t} \quad \dots (10)$$

If we apply Ohm's law,  $J(Z) = \sigma(Z) E$  and assuming a solution to equation (10) of the form  $E = E_0 \exp(-ikz + i\omega t)$ , eqn. (10) is now written as

$$-\nabla^2 \mathbf{E} = \frac{\omega^2}{c^2} \left( \epsilon_{\infty} - \frac{4\pi\sigma(z)i}{\omega} \right) \mathbf{E} \quad \dots (11)$$

For the semi infinite crystal  $0 < Z < \infty$ , then dielectric constant is

$$\epsilon(Z) = \left( \epsilon_{\infty} - \frac{4\pi\sigma(z)i}{\omega} \right) E \quad \dots (12)$$

In the THz frequency range, the propagation of electromagnetic waves through doped semiconductors such as silicon is well characterised by the Drude model which assume that the collision frequency  $\frac{1}{\tau}$ , of the free electron in the doped silicon is negligible compared to THz frequencies, that is  $\omega\tau \gg 1$ . From experimental data for the direct current conductivity versus dopant density, the scattering time  $\tau$  can be estimated from

$$\sigma_{dc} = \frac{he^2\tau}{m} \quad \dots (13)$$

For doped silicon with  $N_e \sim 10^{18} \text{ cm}^{-2}$ ,  $\frac{1}{\tau} \sim 6.46 \text{ MHz}$  [10]. If we neglect collisions, the dielectric constants can be expressed as

$$\epsilon(Z) = \epsilon_{\infty} - \frac{\omega_p(z)^2}{\omega^2} \quad \dots (14)$$

where  $\omega_p^2 = 4\pi Ne^2 / m$  is the plasma frequency. The index of refraction can be expressed as

$$n(z) = \sqrt{\epsilon_{\infty} - \frac{\omega_p(z)^2}{\omega^2}} \quad \dots (15)$$

By using eqn. (12) and (14) we can express eqn. (11) as

$$-\nabla^2 \mathbf{E} + \frac{\omega_p(z)^2}{c^2} \mathbf{E} = \frac{\omega^2}{c^2} \epsilon_{\infty} \mathbf{E} \quad \dots (16)$$

In one dimension eqn. (16) may be written as

$$-\frac{\nabla^2 E}{\partial z^2} + \frac{\omega_p(z)^2}{c^2} E = \frac{\omega^2}{c^2} \epsilon_{\infty} E \quad \dots (17)$$

If we compare eqn. (17) to eqn. (4), we see that the eigenfunction  $\psi$  and electric field are analogous. The quantity  $\frac{\omega^2}{c^2}$  takes on the role of the eigenvalue  $\frac{2me}{h^2}$  of eqn. (4). The condition for travelling wave solution for photonic band-gap materials is given by eqn. (5) with

$$K = \frac{\omega}{c} \sqrt{\epsilon_{\infty}} \quad \dots (18)$$

and

$$Q = \frac{1}{c} \sqrt{\omega_p^2 - \omega^2 \epsilon_{\infty}} \quad \dots (19)$$

where  $\omega_p$  is the plasma frequency of the doped layers. We note that the similar form of the eqn. (18) and (4) are results of particular form of the frequency dependent dielectric constant, that is, the  $\omega_p^2 / \omega^2$  term in eqn. (16). If  $Q$  is imaginary eqn. (5) is still the solution, of the photonic crystal [9, 11] with  $Qb \rightarrow \cos|Q|bd$  and

$$\frac{Q^2 - K^2}{2QH} \sin \frac{|Q^2| + |k^2|}{2|Q|K} \sin |Q|b \quad \dots (20)$$

For typical application of the Kronig-Penney model to crystals, the value of  $Q$  in eqn. (7) is real because the potential barriers is higher than the energy of the moving particles. In order to make  $Q$  real in eqn. (21)  $\omega_p^2 > \omega^2 \epsilon_{\infty}$ . In this regime, the electromagnetic frequency is below the plasma frequency cutoff for free electrons in the doped layers. So the wave function is exponentially damped in these regions. This condition is analogous to that of a solid state system for which the energy of the particle is smaller than the barrier potential ( $\epsilon - U < 0$ ).

## DISPERSION RELATION

We attempted to apply the realistic parameters to eqn. (19) and produce a dispersion relation. The photonic structures, as stated earlier, is comprised of a stack of alternating doped and un-doped silicon layers. The resistivity of the doped silicon is  $0.023 \Omega \text{ cm}$ , which

corresponds to a carrier concentration of  $N = 10^{18} \text{ cm}^{-3}$ . The refractive index,  $n$ , is plotted against frequency in fig. 2 using eqn. (17) to illustrate which frequency are solely absorbed by the doped layers, that is the operating range. The un-doped layers have negligible carrier concentration so that the index of refraction is dominated by the bounded charges. In order for the index of the doped layers to be imaginary,  $\omega_p^2 > \omega^2 \epsilon_\infty$ , the frequency of the incident light must be less than  $\sim 2.8 \text{ THz}$ . A plot of the arc-cosine of the left hand side of the eqn. (5) versus frequency yields the dispersion relation of the crystal, as shown in fig. 3.

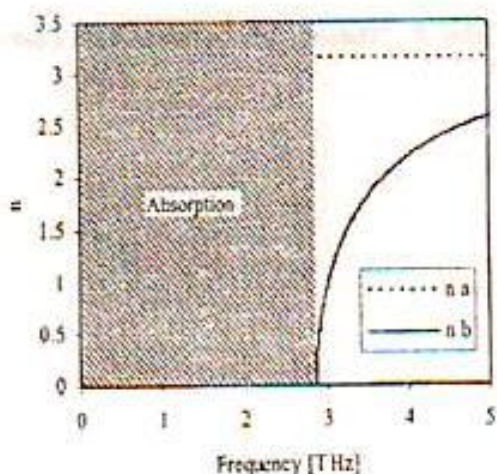


Fig. 2

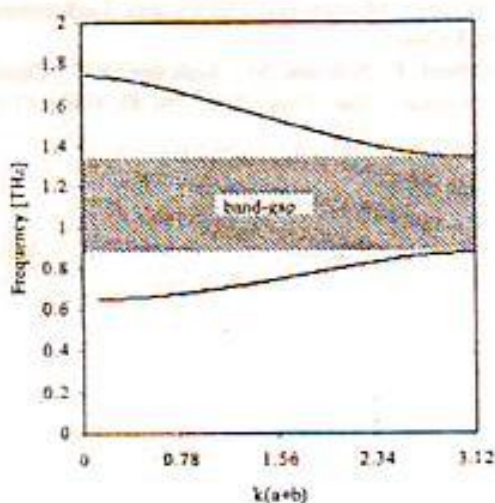


Fig. 3

## CONCLUSION

An analytical solution in THz region has been formulated for photonic band-gap structures analogous to Kronig-Penney model of electronic band-gaps by transforming Maxwell's eqn. in equivalent form of Schrodinger equation assuming a Drude like frequency dependent conductivity of free carriers in alternating layers of a semiconductor photonic band-gaps materials.

## REFERENCES

1. Joannopoulos, J.D., Meade, R.D. and Winn, J.N., *Photonic Crystals: Road from Theory to Practice* (Princeton University Press, Princeton, NJ) (1995).
2. Joannopoulos, J.D., Meade, R.D. and Winn, *Photonic Crystals : Molding the Flow of Light* (Princeton University Press, Princeton, NJ) (1995).
3. Eggert, J.H., "One-dimensional lattice dynamics with periodic boundary conditions : An analog demonstration," *Am. J. Phys.*, **65**, 108-116 (1997).
4. Griffiths, J.H.D.J. and Steinke, "Waves in locally periodic media," *Am. J. Phys.*, **69**, 137-154 (2001).
5. Kronig, R. de, E. and Penney, W.G., "Quantum mechanics of electrons in crystal lattices," *Proc. R. Soc., London, Ser. A* **130**, 499 (1931).
6. Kittel, C., *Introduction to Solid State Physics*, 7th ed. (Wiley, New York) (1996).
7. Ashcroft, N.W. and Mermin, N.D., *Solid State Physics* (Saunders College, New York) (1976).
8. Dowling, J.P. and Bowden, C.M., "Atomic emission rates in inhomogeneous media with applications to photonic band structures," *Phys. Rev., A* **46**, 612622 (1992).
9. John, S. and Wang, J., "Quantum electrodynamics near a photonic band gap: Photon bound states and dressed atoms," *Phys. Rev. Lett.*, **64**, 2418, 2421 (1990).

# Analysis of Surface Wave Propagation in PBG Structure

Dr Prakash Nayak \* & Dr. Dhirendra Kumar \*\*

28 \*Principal Investigators ( UGC – MRP ) & Head, P. G. Department of Physics, R. K. College, Madhubani. E Mail – [prakashnayak.17@gmail.com](mailto:prakashnayak.17@gmail.com).

\*\* Project Fellow, UGC – MRP, P. G. Department of Physics, R. K. College, Madhubani. E mail – [k.dhirendra17@gmail.com](mailto:k.dhirendra17@gmail.com).

## Abstract :-

Photonic band gap (PBG) structures are periodic structures in which optical waves are forbidden in certain frequency bands. Extensive investigations have been conducted to translate and apply this property to the microwave and millimeters -wave domain and several applications at microwave frequencies have been developed including antenna substrate, resonant cavities and filters. In this paper surface wave propagation along the planar PBG lattice has been investigated. For this two dielectric slabs clad with the planar PBG structures – one on a conductor backed slab and the other on a bare dielectric slab were used. The results have been discussed.

## Introduction :-

PBG structures can be one-, two-, or three dimensional periodic structures. Due to the analogy between electromagnetic wave propagation in periodic structures and electron wave propagation in crystal, PBG structures find application in both optics and microwave regime[1,2]. Electromagnetic crystals at microwave frequencies can be realized by scaling the structures used at optical frequencies. For examples, by micromachining holes in dielectric slab, a two – dimensional periodic variation of the material refractive dielectric is achieved. Many attempts to reduce the physical size of these structures have been reported in literature. One such method is to use metallo – dielectric structures [ 3,4 ]. The basic idea here is the introduction of a periodic network of LC – element to shorten the wavelength of the propagating wave. An effective example of metallo – dielectric crystal is given by the high impedance ground plane described in [5], which is employed to improve patch antenna performance [6,8]. It is comprised of a grounded dielectric slab periodically loaded with square lattice of square metallic pads, realizing a 2D periodic network of capacitors. Each pad is connected to ground through one via at its centre which provides the inductive parts of the LC – network.

The above approach, although very effective, requires a non – planar fabrication. Recent research efforts focus on development of planar electromagnetic crystals that do not require vias and that can be easily integrated in microwave and millimeter wave circuits.

In the present paper analysis of surface wave propagation in two dimensional PBG structure in two different situations have been done and results for basic properties like stop band, pass band and cut off frequencies have been compared.

## Surface waves in compact crystals periodically distributed in two dimensions

To investigate surface wave propagation along two – dimensional PBG lattice, two dielectric slabs clad with the two dimensional PBG structure were used – one on a conductor – backed slab and the other on a bare dielectric slab. In both cases, a stop band for surface wave propagating along the structure still appears when the condition  $\beta a = \pi$ , is satisfied. However, the presences of the LC – networks reduce the wavelength of surface wave, so that the period of the planar PBG is significantly smaller than half – wavelength in free space.

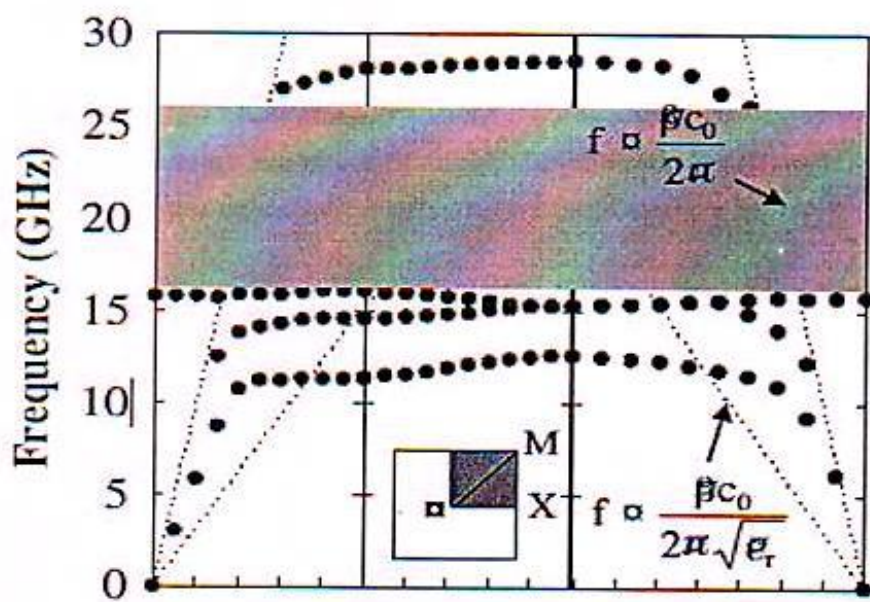
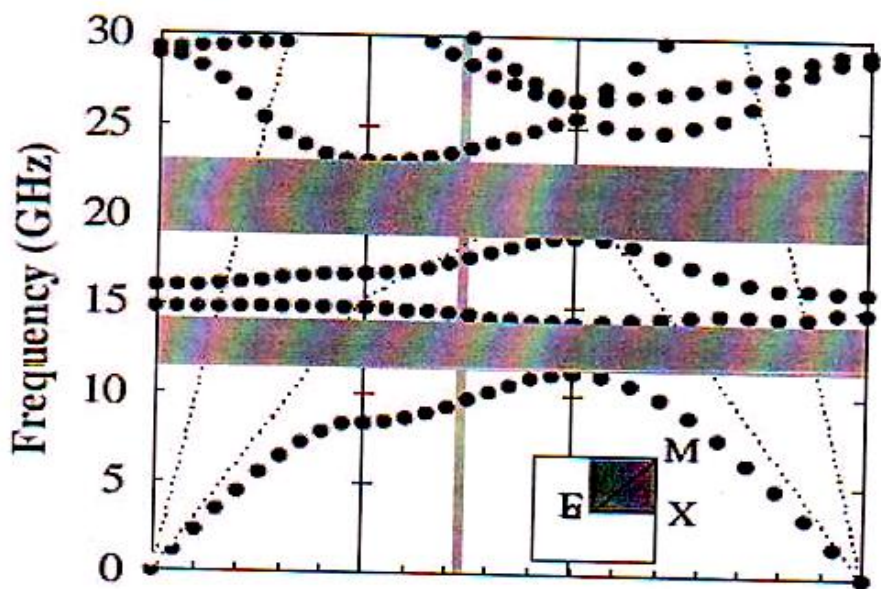


Fig. 1: Dispersion diagram of planar PBG structures on a bare dielectric slab.



**Fig. 2** : Dispersion diagram of planar PBG structures on a conductor- backed dielectric slab.

Fig. 1 shows the dispersion diagram for the two different cases of planar PBG used on a bare dielectric slab and fig. 2 on a conductor backed dielectric slab . Several differences have been found between the two figures. First, while the planar PBG on a bare dielectric slab presents a wide stopband between the third and fourth mode in the frequency range 16.1 to 26.1 GHz, the planar PBG on a conductor – backed dielectric slab has two stop bands. The first stop band is between the first and second mode, spanning the frequency range 11.3 and to 14.1 GHz; the second is between the third and fourth modes in the frequency range 18.9 to 23 GHz. Moreover, the second and fourth modes of the conductor- backed dielectric slab planar PBG do not show any cut- off frequency as seen instead for the second and fourth modes of the bare dielectric slab planar PBG. The fundamental mode of both structures is a TM- like mode with a strong longitudinal component o the electric field. Computations shows that, as expected, the effective dielectric constants of the fundamental mode is higher in the case of conductor- backed dielectric slab planar PBG. This is due to the fact that the backed conductor confines the electric fields inside the high permittivity region. The second and third modes for both cases are predominately TE modes with a strong transverse component of the electric field.

## Results and Discussions

The nature of wave propagation along the microstrip based planar PBG structure can be further elucidated by considering the Brillouin zone [7, 9, 10] of the lattice as depicted in figure (1). The X- section describes mode propagation along the planar PBG structures in a direction parallel to the primitive vectors of the square lattice. The first TM- like mode has a cut- off frequency at the X- point of 11.4 GHz for the case of planar PBG on a bare

dielectric slab, and 8.4 GHz for the case of planar PBG on a conductor- backed dielectric slab. The measured cut- off frequency for the microstrip guided mode is 10 GHz. As expected, this value is between the two extreme cases of planar PBG on a bare and conductor backed dielectric slab.

## References:-

1. Yablonovitch E., "Photonic band- gap structures" *J. Optical Soc. America B*, Vol 10, pp. 283- 295, 1993.
2. Joannopoulos J. D., Meade R. D., and Winn J. N., "Electromagnetic modeling for microwave imaging of cylindrical buried inhomogeneities," *Photonic crystals* , Princeton Univ. Press, Princeton , NJ, 1995.
3. Gautheir G. P., Courta A. and Rebbeiz G. M., "Microstrip antennas on synthesized low dielectric constant substrates" *IEEE Trans. Ants. And propag.* , vol. 45, no 8, pp. 1310- 1314, 1995.
4. Brown E. R. and McMahon O. B., "Large electromagnetic stop bands in metallocdielectric photonic crystals," *Applied Phys. Letters*, Vol. 67, No. 15, pp. 2138- 2140, 1995.
5. Sievenpiper D., Yablonovitch E., Winn J. N., Fan S., Villeneuve P. R., and Joannopoulos J. D., "3D metalloc- dielectric photonic crystals with strong capacitive coupling between metallic islands," *Physical Review Letters*, vol. 80, No 13, pp. 2829- m2832, 1998.
6. Sievenpiper D. and Yablonovitch E., "Eliminating surface currents with metallocdielectric photonic crystals," *IEEE MTT- S Symp. Dig.*, pp. 663- 666, Baltimore, MD, 1998.
7. Qian, Y., Sievenpiper D., Radisic V, Yablonovitch, E., and Itoh, T "A novel approach for gain and bandwidth enhancement of patch antennas," *IEEE RAWCON . Symp. Dig.*, pp. 221- 224, Colorado Springs, CO, 1998.
8. Karmakar, N. C. and Mollah M. N., "Investigations into Non-uniform Photonic bandgap Microstrip Line Low Pass Filters" *IEEE Trans. Microwave Theory Techniques*, vol. 51, no.2, pp. 564-572, 2003.
9. Skivesen N, Tetu A, Kristensen M, Kjems J, Frandsen LH, Borel PI, Photonic-crystal waveguide biosensor, *Opt Express*, Vol. 15 No., pp63169–3176 (2007).
10. H.-I. Lee, "Wave classification and resonant excitations in lossy metal-dielectric multilayers," *Photonics Nanostruct. Fundam. Appl.* 8(3), 183–197 (2010).



## Study of the Effect of PBG Structure on the Performance of Printed Antenna

Dr. Prakash Nayak\* and Dr. Dhirendra Kumar\*\*

\*Principal Investigator (UGC – MRP) and Head, P.G. Deptt. Of Physics, R. K. College, Madhubani. E-mail-prakashnayak.17@gmail.com.

\*\* Project Fellow (UGC – MRP), P. G. Deptt. Of Physics, R. K. College, Madhubani. E-mail-k.dhirendra17@gmail.com.

### Abstract

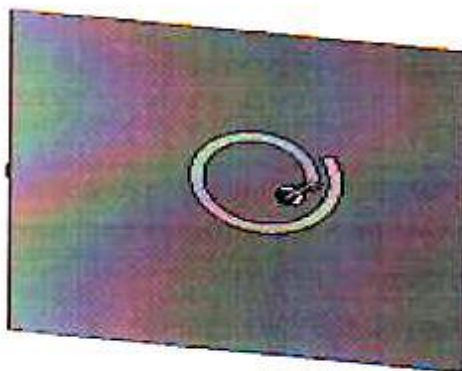
A substrate with relatively high permittivity is used to reduce the size of radiating elements. At the same time to attain large bandwidth substrate should be thick. As a result, lot of power is lost to surface waves and waves trapped in dielectric. This phenomenon increases the coupling between elements which strongly affects the performance of antenna. In this paper we have shown by simulated results that performance of printed array antenna is significantly improved by using a Photonic Band Gap ( PBG ) substrate instead of standard substrate. As a first step towards realization of an array antenna two printed spirals have been put next to each other and simulation have been made with and without PBG structure. The improvement on the radiation pattern caused by the presence of PBG structure was found to be very significant.

**Keywords :** Photonic Band Gap (PBG ), Array Antenna, Substrate, Surface waves.

## Introduction

High speed data transmission requires wide bandwidth. Also for low angle scanning the radiating elements should be small enough to be placed close to each other in order to minimise the appearance of grating lobes. Thus a substrate with high permittivity should be used to sufficiently reduce the size radiating elements. At the same time for relatively large bandwidth the substrate should be thick enough. Consequently the array antenna, which finds many applications, needs then to be manufactured on a thick dielectric having a high permittivity. In this type of substrate lot of power is lost due to surface wave generated in the dielectric and the coupling between elements strongly affects the performance of the antenna (1,2).

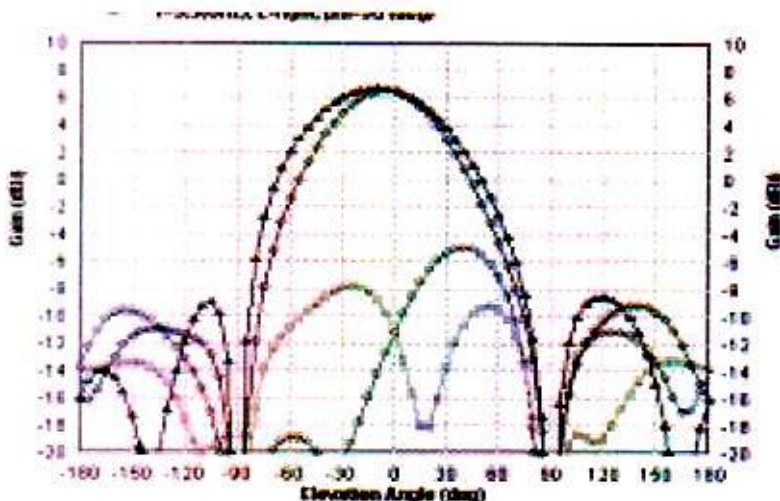
In this paper a metallo- dielectric photonic band gap structure has been used to work on the same substrate as one supporting the radiating element. The radiating element used for this study is a printed spiral fed by a probe. This element is interesting because it furnishes a good matching and a natural circular polarisation over a fairly large bandwidth. This bandwidth, which is in the order of 10% is largely sufficient for this applications. The printed circular spiral has a circumference of a wavelength and is placed around 0.2 wavelength of the considered medium above a perfect electric conductor ( Fig. 1).



Figure(1)

By tuning the length of the spiral, circular polarization can be obtained. The circular polarization, right hand or left hand, depends on the winding direction of the spiral. The considered spiral produces a right hand circular polarization. A printed spiral has been designed to work at 5.5 GHz. The spiral is printed on top of a substrate of thickness 6.1 mm and with relative permittivity 2.2. The spiral is fed from a microstrip line with a help of a probe. The antenna exhibits a bandwidth of 500 MHz centered around 5.5 GHz with a return

loss lower than  $-17$  dB. Over this bandwidth the boresight cross polarization remain close to  $-15$  dB. The radiation pattern for the central frequency  $5.5$  GHz is shown in Fig. (2).



Figure(2)

Some high level of cross polarization out of boresight can be observed. The radiation efficiency at  $5.5$  GHz. is  $69\%$ . The effect of the PBG structure on the performance of the printed spiral radiating element has been evaluated. The previous antenna has been embedded inside the PBG structure. Because of computational limitations, the antenna has been analysed with only one row of PBG cell surrounding it. We clearly see the improvements on the radiation pattern due to PBG structure in fig. 3.

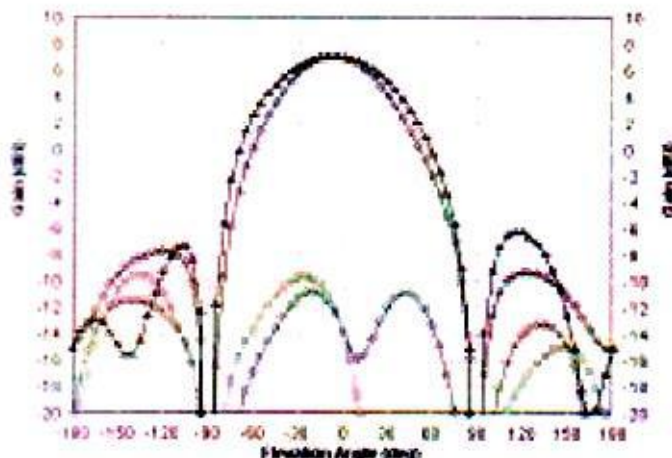


Figure (3)

The pattern is more symmetric and the level of cross polarisation is lower than without PBG structure. The gain has increased by almost  $1$  dB and efficiency is now  $86\%$  instead of  $69\%$  without the presence of the PBG structure.

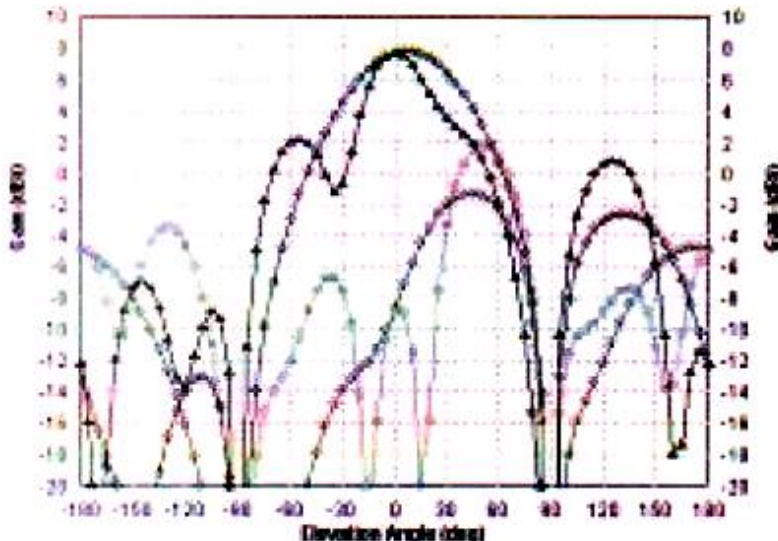
## Realisation of array antenna

The first step towards the realisation of an array antenna is to check the interaction between two adjacent elements(3,4). Two printed spiral have been put next to each other with a distance of 0.6 lambda between them. Simulations have been made with or without PBG structure using HFSS software. When the PBG is present there is one row of cells around each spiral. Therefore there are two rows of cells between them. The isolation between the two spirals, with or without is presented in table 1.

Frequency	5.25 GHz	5.50 GHz	5.75 GHz
Isolation (dielectric)	- 19.3 dB	- 18.4 dB	- 16.1 dB
Isolation (PBG)	- 23.9 dB	- 23.2 dB	- 22.2 dB

Table 1

Despite of a small no. of PBG cells around each spiral, the improvement on the radiation pattern caused by the presence of the PBG structure are very significant shown in figure(4) and figure (5).



Figure(4)

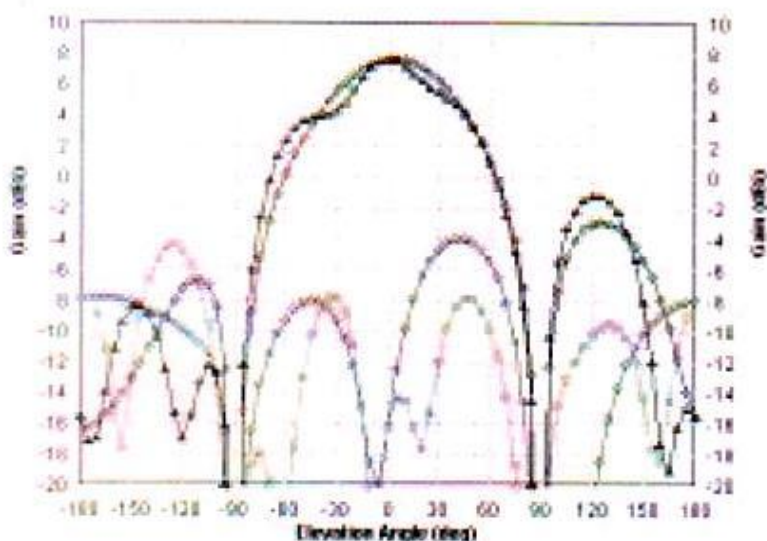


Figure (5)

## Conclusion

The simulation results indicate that the use of PBG substrates instead of a standard substrate significantly improves the performance of printed antenna. The use of the proposed PBG structure seems very promising to reduce the coupling and diffraction problems caused by surface waves in array antennas. The investigation carried out for low profile array antenna using only one row of PBG cell surrounding it, points out that in the manufactured structures using more PBG cells will further improve the performance.

## References

- (1) Sievenpiper, D., Zhang, L., Broas, R. F. J., Alexopolous, N. G. and Yablonovitch. E., " High – impedance electromagnetic Surface with a Forbidden frequency band", IEEE Trans. On MTT, Vol. 47, No. 11.(1999).
- (2) Gonzalo, R., Maagt. P. de and Sorolla. M., " Enhanced Patch- Antenna Performance by Suppressing Surface waves using Photonic Band Substrates ", IEEE Trans. On MTT, Vol. 47, No. 11(1999).
- (3) Hui, H. T., Bialkowski, E. and Lui, H. S., 'Mutual coupling in antenna Arrays', International Journal of Antenna and Propagation, Vol. 10, PP. 2(2010).
- (4) Wang. X., Zhang, M. and Wang, S. -J, " Practicability Analysis and Applications of PBG structures on cylindrical conformal Microstrip Antenna and Array" PIER, Vol. 115, pp. 495-507(2011)

## Photonic Crystal as a Substrate for Patch Antennas

PRAKASH NAYAK and DHIRENDRA KUMAR

Department of Physics, R. K. College, Madhubani.

### Abstract

In this paper Photonic crystal structures is used as substrate in order to mitigate the effect of the surface wave mode propagation. The case of a single antenna has been studied. A comparison between a conventional substrate based patch and a patch with a photonic crystal as substrate has been performed. Simulation was done with HFSS software. Improvements in all the main parameters of the antenna were obtained when using a photonic crystal. The frequency dependence of the radiation patterns is significantly reduced when using a photonic crystal as substrate. This opens the door to design new devices with thicker substrates and higher dielectric constant without losing performance by the undesired excitation of the surface wave modes.

### Introduction

The microstrip patch has been a popular antenna for many years, as it is low profile, robust, conformable if required and inexpensive to manufacture [Bahl et. al 1980, James et. al 1981 & 1989, Balanis 1997]. However, patch antenna designs can have some operational limitations such as restricted bandwidth of operation, low gain and a decrease in radiation efficiency due to surface wave losses. Thickening the substrate increases the operational bandwidth, but at the same time increases the excitation of substrate modes and a trade-off must be performed. The concept of photonic bandgap materials can have a significant influence on the outcome of such a trade off.

The photonic bandgap materials introduced in the late eighties allow to control the emission and propagation of electromagnetic waves into a dielectric substrate to an extent that was previously not possible [Joannopoulos et.al 1995, de Maagt et. al 1999, Scherer et. al 1999]. Although many applications have initially been proposed in the field of optics, the scalability of these structures opens up the possibility of using them in the microwave regime. In this frequency range, photonic bandgap materials have attracted a lot of attention as substrates for antennas [ Brown et. al 1993, Sigalas et. al 1996 , 1997 & 1999, Yang et. al 1997, Quian et. al 1999, Agi et. al 1999, Gonzalo et. al 1999 & 2000, Colburn et. al 1999]. The basic idea is to match the operational bandwidth of the antenna with the bandgap of the photonic crystal. The utilization of a photonic crystal substrate, instead of the original bulk substrate, has shown to reduce the excitation of surface wave modes, and as a consequence improves the antenna radiation efficiency, reduces the side lobe level and mitigates the problems related to coupling.

In this paper, the design of a photonic crystal as a substrate for patch antennas is discussed. The performance of a single patch on a conventional substrate is compared to that of a patch on a photonic crystal substrate.

### Design of the Photonic Crystal and Microstrip Antenna

Different kinds of PC structures can be used as substrates [Meade et. 1993, Baba et. al 1995, Casagne et. al 1996, Johnson et. al 1999], the proposed structure is a square lattice of air columns with a radius  $r$  and lattice constant  $a$  drilled in a dielectric medium with a dielectric constant  $\epsilon_r = 10$ , figure 1. The advantage of using this configuration versus other possibilities is a higher number of holes per wavelength [Gonzalo et. al 1999].

After defining the basic photonic crystal geometry, the dispersion relation for a normal incident plane wave can be calculated. The “gap map” for the structure is obtained by keeping the dielectric constant fixed, sweeping the  $r/a$  ratio and recording the width of the gap [Joannopoulos et. al 1995]. This gap map then allows us to choose the  $r/a$  value that maximises the available photonic band gap for the desired frequency of operation. Using these maps and taking a working frequency of 15 GHz, the lattice constant  $a$  can be obtained.

There are different possibilities, but the selection criteria will be governed by minimising the total device size. By ensuring the only surface mode in propagation will be the TM0 [22], one only has to focus on the TM polarisation gap-map. With these two premises, a value for  $r/a$  of 0.48 was selected. Together with a normalised frequency of 0.3 this gives a physical lattice period of 6 mm and a column radius of 2.88 mm.

**Keywords :** Photonic crystal structures, di- electric constant, substrate, HFSS software.

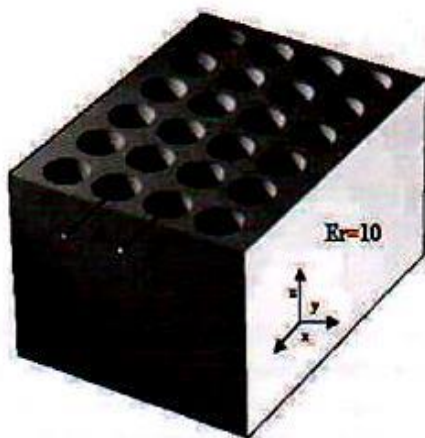


Figure 1

In the patch antenna configuration was fed using the aperture coupling method. This feeding scheme provides several advantages over other arrangements, primarily due to the physical separation between the radiating region and the feeding network. Aperture coupling provides the freedom of choosing two different substrates, according to practical or technological requirements. With respect to coplanar waveguides feeding, the present solution provides radiation pattern regularity and polarisation purity [Bahl et. al 1980, James et. al 1981 & 1989, Balanis 1997].



Figure 2(a)

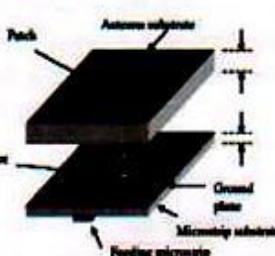


Figure 2(b)

The geometry of the patch antenna is shown in Figure 2(a) & 2(b); it has a width  $W$  of 4.6 mm and a length  $L$  of 1.5 mm. The upper/lower antenna/microstrip substrate is 1.27 mm/0.635 mm thick, respectively.

The transmission line designed to feed the patch antenna has a width  $W_f$  of 0.635 mm and a stub length  $L_s$  of 2.286 mm, measured from the center of the patch antenna, to match the input impedance of the antenna [Cocciali et. al 1999]. The slot in the ground plane to couple the power from the transmission line to the patch antenna has an H shape. The dielectric constant is 10.2/0.2 for both substrates and the total substrate size is 60×60×1.27 mm. The antenna is placed at the central position of the substrate.

According to the design guidelines given in [James et. al 1979], the surface wave excitation becomes noticeable when  $h/\lambda > 0.03$  for  $\epsilon_r H > 10$ , with  $h$  the height of the dielectric substrate. Following this rule of thumb, there should be significant excitation of surface wave modes for the selected thickness of the antenna substrate.

### Simulation and Discussion

The simulation of both configurations was done by using HFSS software. The simulated input return loss is shown in figure 3.

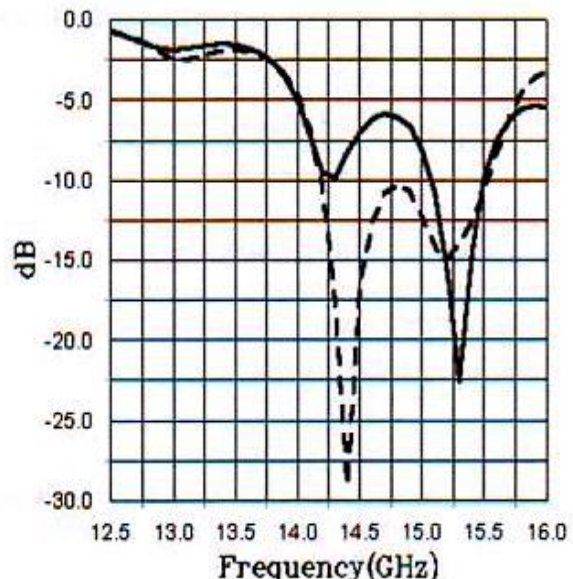


Figure 3

Both curves are quite similar, only a small shift for the Photonic Crystal substrate is observed. The obtained bandwidth, defined for an  $S_{11}$  of -7.5 dB, is about 8% for both cases.

The simulated radiation patterns are depicted in Figure 4(a) and 4(b). These patterns are shown for a frequency of 15.2 GHz for which both antennas have the same  $S_{11}$ . The improvements obtained by using the Photonic Crystal substrate are obvious.

The size of the substrate is such that, in theory, the surface wave mode is added in counter-phase for the conventional patch antenna, resulting in a very low value for the gain in boresight direction. This effect of surface waves is nearly completely eliminated by the photonic crystal substrate, leading to a smooth radiation pattern. This gain value in boresight is increased by more than 6 dB, while the back and side radiation has been reduced considerably. The front-back ratio has improved by 6 dB.

## Photonic Crystal as a Substrate for Patch Antennas

The reduction in surface waves as a result of the photonic crystal material is also clear from the surface plot of the electric field. Finally, the radiation patterns in the E-plane (the plane in which the surface waves are more pronounced) are presented in Figure 4(a) and 4(b) for several frequencies. The frequencies go from 13.5 GHz to 16 GHz in steps of 0.5 GHz. The pattern for the conventional case (Figure 4(a)) is varying strongly as a function of frequency due to the presence of substrate modes. On the other hand the frequency dependence is reduced while using a photonic crystal substrate, indicating that the surface wave mode has been mitigated in the frequency range of operation (about 13.5 to 15.5 GHz).

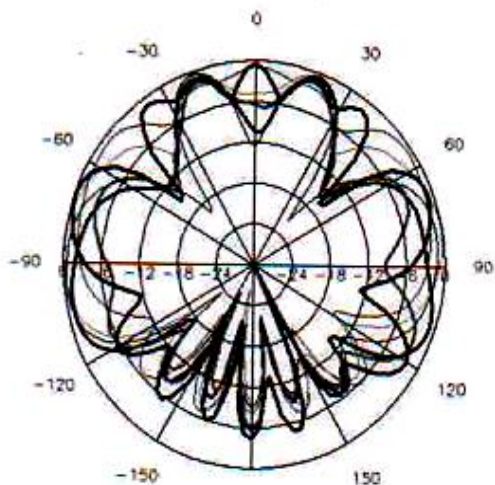


Figure 4(a)

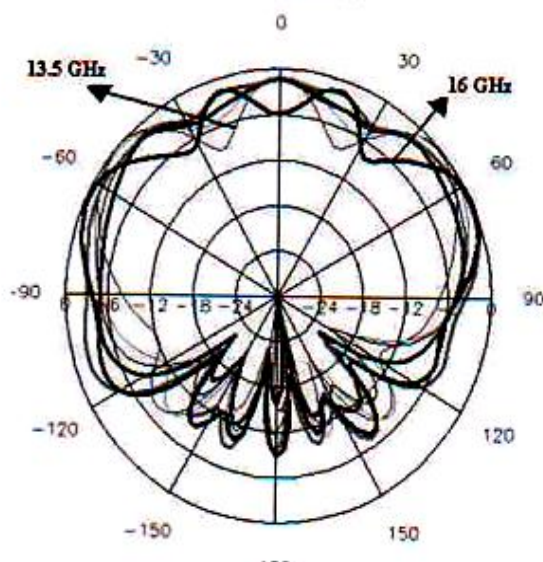


Figure 4(b)

It should be noted that the cut at 16 GHz (thick line) shows a deep ripple in both cases because it lies outside the gap of the photonic crystal.

## Conclusion

Simulations of a patch antenna on top of a conventional and a Photonic Crystal substrate have been presented. Substantial improvements by using Photonic Crystal substrates have been obtained.

At the design frequency, the patch antenna on a Photonic Crystal has more directivity, less side and back radiation and a smoother pattern. The gain in the boresight direction increases significantly.

The radiation patterns show little dependence with frequency using a PC substrate. On the other hand using a conventional substrate clear frequency dependence is present.

The ability of the Photonic Crystal substrate to reduce the surface wave mode propagation has been clearly proven. This opens the door to design new devices with thicker substrates and higher dielectric constant without losing performance by the undesired excitation of the surface wave modes.

## Acknowledgment

Author gratefully acknowledge to U. G. C. ( New Delhi ) for granting a Major Research Project.

## References

1. Agi, K., J. Malloy, E. Schamiloglu, M. Mojahedi, and E. Niver, 1999. Integration of microstrip patch antenna with a two-dimensional photonic crystal substrate, Electromagnetics Special Issue: Theory and Applications of Photonic Band-Gap Materials, 19(3): 277-290.
2. Baba, T. and T. Matsuzaky, 1995. Theoretical calculation of photonic gap in semiconductor 2-dimensional photonic crystals with various shapes of optical atoms, J. Appl. Phys., Vol. 34, 4496-4498, Aug. 1995.
3. Balanis, C. A., 1997. Antenna Theory. Analysis and Design, Second edition, John Wiley & Sons, Inc.
4. Bahl, I. J. and P. Bhartia, 1980, Microstrip Antennas, Artech House.
5. Brown, E. R., C. D. Parker, and E. Yablonovitch, 1993. Radiation properties of a planar antenna on a photonic-crystal substrate, Journal of Optic Soc. Am. B., 10(2): 404-407.

6. Casagne, D., C. Jouanin, and D. Bertho, 1996. Hexagonal photonic band-gap structures, *Physical Review B*, 53(11): 7134–7142, Mar.
7. Cocciali, R., F. Yang, K. Ma, and T. Itoh, 1999. Aperture-coupled patch antenna on UC-PBG substrate, *IEEE Transactions on Microwave Theory and Techniques*, Vol. 47(11).
8. Colburn, J. S. and Y. Rahmat-Samii, 1999. Patch antennas on externally perforated high dielectric constant substrates, *IEEE Transactions on Antennas and Propagation*, 47(12): 1785–1794., Dec.
9. Collin, R. E., 1999. *Field Theory of Guided Waves*, Second Edition, IEEE Press.
10. de Maagt, P. J. I., R. Gonzalo, and A. Reynolds, 1999. PBG Crystals: periodic dielectric materials that control EM wave propagation, *Microwave Engineering Europe*, 35–43.
11. Gonzalo, R., P. J. I. de Maagt, and M. Sorolla, 1999. Enhanced patch antenna performance by suppressing surface waves using photonic band-gap structures on *IEEE Transactions Theory Microwave and Techniques*, Mini-Special Issue on Electromagnetic Crystal Structure, Design, Synthesis, And Applications, 47(11): 2131–2138.
12. Gonzalo, R., B. Martinez, P. J. I. de Maagt, and M. Sorolla, 2000. Improved patch antenna performance by using photonic band-gap substrates, *Microwave and Optical Technology Letters*, 24(4) : 213–215.
13. James, J. R., P. S. Hall, and C. Wood, 1981. *Microstrip Antenna. Theory and Design*, Peter Peregrinus Ltd.
14. James, J. R. and P. S. Hall, 1989. *Handbook of Microstrip Antennas*, IEE Peter Peregrinus Ltd.
15. James, J. R. and A. Henderson, 1979. High-frequency behaviour of microstrip open-circuit terminations, *IEE J. Microwaves, Optics and Acoustics*, 3: 205–218.
16. Joannopoulos, J. D., R. D. Meade, and J. N. Winn, 1995. *Photonic Crystals. Molding the flow of light*, Princeton University Press.
17. Johnson, S. G., S. Fan, P. R. Villeneuve, and J. D. Joannopoulos, 1999. Guided modes in photonic crystal slabs, *Physical Review B*, Vol. 60(8): 5751–5758.
18. Meade, R. D., A. M. Rappe, K. D. Brommer, and J. D. Joannopoulos, 1993. Nature of photonic band gap: some insights from a field analysis, *J. Opt. Soc. Am. B*, 10(2).
19. Scherer, A., T. Doll, E. Yablonovitch, H. O. Everitt, and J. A. Higgins, 1999. Mini-special issue on electromagnetic crystal structures, design, synthesis, and applications, *IEEE Microwave Theory and Techniques*: 47(11).
20. Sigalas, M. M., R. Biswas, K. M. Ho, W. Leung, G. Tuttle, and D. D. Crouch, 1999. The effect of photonic crystals on dipole antennas, *Electromagnetics Special Issue: Theory and Applications of Photonic Band-Gap Materials*, 19(3): 291–303.
21. Sigalas, M. M., R. Biswas, K. M. Ho, W. Leung, G. Tuttle, and D. D. Crouch, 1999. The effect of photonic crystals on dipole antennas, *Electromagnetics Special Issue: Theory and Applications of Photonic Band-Gap Materials*, 19(3): 291–303.
22. Sigalas, M. M., R. Biswas, and K. M. Ho, 1996. Theoretical study of dipole antennas on photonic band-gap materials, *Microwave and Optical Technology Letters*, 13(4): 205–209.
23. Sigalas, M. M., R. Biswas, Q. Li, D. Crouch, W. Leung, R. Jacobs-Woodbury, B. Lough, S. Nielsen, S. McCalmont, G. Tuttle, and K. M. Ho, 1997. Dipole antennas on photonic band-gap crystals—experiment and simulation, *Microwave and Optical Technology Letters*, 15(3): 153–158.
24. Quian, Y., R. Cocciali, D. Sievenpiper, V. Radisic, E. Yablonovitch, and T. Itoh, 1999. A microstrip patch antenna using novel photonic band-gap structures, *Microwave Journal*, 66–76.
25. Yang, D., N. G. Alexopoulos, and E. Yablonovitch, 1997. Photonic band-gap materials for high-gain printed circuit antennas, *IEEE Trans. on Antenna and Propagation*, 45(1).

# **State of Research on Using PBG Components in Radio Frequency (RF) Antenna System**

**Dr. Prakash Nayak\* and Dr. Dhirendra kumar\*\***

\* Principal Investigator, UGC-MRP & Head, P.G. Deptt. of Physics, R.K. College, Madhubani, 847211 (Bihar).

\*\* Project Fellow, UGC- MRP, P.G. Deptt. of Physics, R.K. College, Madhubani, 847211(Bihar).

## **Abstract :**

In this paper a brief survey of recent trends and developments of radio frequency (RF) antenna – oriented PBG research beginning with the use of PBG substrates for planar antenna and concluding with an examination of PBG structures as antenna reflector is presented .While PBG substrates and reflectors are useful for improving antenna gain, efficiency and directivity; more research to resolve question concerning both the effect of a PBG substrate on an antennas pattern shape and the sensitivity of antenna performance to placement relative to PBG lattice have been suggested.

## **Keywords:**

Radio-Frequency, PBG substrate, Planar Antenna, Antenna Reflector, PBG Lattice.

## Introduction:

In 1987, a laser researcher at Bell Communication Research (Bellcore) suggested that an artificial analog of a natural crystal structure might function as an omnidirectional spatial filter for EM radiation (Yablonovitch, 1987). Since then researchers from such disparate backgrounds as quantum physics, computational electromagnetic, material sciences, and electrical engineering have come to collaborate in the development of a growing subject known as photonic band gap (PBG). Simply defined, a PBG crystal is a man made object with a periodic structure such that it prevents the propagation of certain EM modes in all possible direction within its bulk. It can be dielectric, metallic or a mix of both. Properly designed it can have the same degree and type of controllability for EM wave propagation that a doped semiconductor has for electronic propagation.

Such a structure could have clearly had a host of uses. In the radio frequency(RF) arena applications might include antenna substrates and reflectors, wave guides high Q -cavities and various low observable applications.

## PBG Materials as Planar Antenna Substrates:

The first major article on antenna applications of PBG materials reported Lincoln Laboratory's use of a planar bow-tie antenna on a photonic crystal substrate fabricated at Bellcore (Brown et al., 1993). The published results showed a dramatic rejection of the antenna radiation from the substrate side of the antenna. The energy dissipated into a uniform dielectric substrate was virtually eliminated when using the PBG substrate. In follow on work, they examined the effects of surface composition and antenna placement on the field pattern of a dipole atop the same type of 'Yablonovite' substrate (Brown et al., 1994). This second experiment showed the same tendency of the PBG substrate to eliminate most of the radiation in the rearward hemisphere. The patterns in the forward hemisphere were significantly different from that of a dipole in free space, with asymmetric spikes appearing in both the E-plane and H-plane patterns. Placing the antenna at different symmetry points on the substrate lattice also changed the patterns, though the authors considered these changes qualitatively minor. The more significant factor was surface composition, apparently because of the different mode structures supported by the two different surfaces tested. After offering the surface mode explanation, the authors still concluded that the problem was "a complex issue involving electromagnetic interaction between metals and dielectrics that may warrant theoretical investigation". Next, University of New Mexico researchers joined the Lincoln Lab effort by designing an ultrawideband (UWB) photonic crystal as a possible broadband antenna substrate (Agi et al., 1994). In this work, they

stacked three photonic crystals with different but overlapping stop bands to achieve a 44% fractional bandwidth centered on 20.5 GHz. This initial group of three antenna-related experiments indicated that PBG substrates might allow significant gain improvement for planar antennas by overcoming the problem of power loss into a homogeneous substrate.

Ellis and Rebeiz at the University of Michigan were the first to report using PBG substrates to improve the commercial viability of a particular type of antenna (Ellis and Rebeiz, 1996). As they pointed out, the tapered slot antenna (TSA) is a form of microstrip antenna usually limited to use on substrates between 0.005 and 0.03  $\lambda$  thick. Throughout much of the millimeter wave band, this results in unreasonably thin substrates. By fabricating the TSA on a dielectric substrate drilled with a hexagonal lattice of holes, Ellis and Rebeiz completely overcame the performance penalties normally associated with mounting a TSA on a thick dielectric substrate. In fact, they also improved antenna directivity by 30%, raised the main beam efficiency 14%, and reduced cross-polarization by 75% compared with a TSA on a normal thin dielectric substrate.

Recently, researchers at UCLA, the University of California at Irvine, and the University of Illinois have presented both measurements and calculations of the behavior of PBG substrates with simple antennas. Cocciali, Deal, and Itoh used a PBG substrate to achieve a 10 dB reduction in the sidelobes caused by surface waves emanating from a microstrip patch (Cocciali et al., 1998). Yang, Alexopoulos, and Yablonovitch calculated a 15 dB power gain over a narrow angular region for a Hertzian dipole with both PBG substrates and superstrates (Yang et al., 1997). They also noticed significant positioning sensitivity of the antenna relative to the PBG lattice. Further computations of substrate and superstrate combinations with a patch antenna predicted a 2-5 dB peak gain over the same antenna backed by a uniform dielectric loaded cavity (Zhang et al., 1998). Clearly, researchers have decided that PBG structures' transmission characteristics are worth exploring for RF sidelobe and backlobe suppression and gain enhancement in microstrip antennas.

### Researches on PBG Materials as Antenna Reflectors:

PBG substrates are integrated directly as the substrates on which microstrip antennas are fabricated. Some researchers have also explored the use of PBG materials as antenna reflectors separated from the radiating element. Such work falls into two broad categories. In the first, completely separate PBG structures serve as planar reflectors for radiating elements. In the second, the PBG reflector and radiating element are both fabricated within the same block of material in a monolithic design.

The 'separate-reflector' category comprises the majority of published work in this area. Kesler et al. at GTRI and Georgia Tech published the first significant article on this implementation of a PBG reflector (Kesler et al.,

1996). This work introduced the effective reflection plane concept. The primary focus was on development and validation of that concept by measuring the patterns generated from dipole antennas placed in front of 2D and 3D dielectric PBG reflectors. Experimental results showed behavior similar to that of the same dipole placed in front of a PEC reflector. These results also agreed well with numerical predictions. This provided an initial validation of the relatively simple ERP model for describing the observable effect of the scattering from a PBG reflector. Smith, Kesler, and Maloney have also used the effective reflection plane model as part of a detailed study of a "woodpile" PBG reflector with a monopole antenna (Smith et al., 1999). This work examines gain, field patterns, and input impedance as functions of frequency and position for the monopole-reflector combination. Both calculation and measurement indicate that the PBG reflector allows a maximum gain of nearly 6 dB relative to the isolated monopole. The ERP model again shows good agreement with more rigorous FDTD calculations.

Sigalas et al. conducted another pair of experiments exploring the effect of antenna positioning relative to a PBG reflector (Sigalas et al., 1997; Leung et al., 1997). Working with another dielectric layer-by-layer or 'woodpile' PBG structure, they experimented with both dipole and slot antennas. For the dipole, calculation and measurement showed significant improvement in directivity for the dipole with reflector versus the free space dipole. Patterns were, however, strongly dependent on two positioning factors. Antenna height and the resulting phase relation between the direct and reflected waves was one factor. Antenna position in the unit cell and its effect on the dipole interaction with the strongly position-dependent E field at the PBG surface was the second factor, though its importance decreased as the antenna was raised further above the reflector (Sigalas et al., 1997). The slot antenna placed on the PBG reflector showed an average gain of 2-3 dB over the free slot for a 14% fractional bandwidth, with positional dependence similar to that shown by the dipole. The slot did hold one distinct advantage over the dipole in that it showed none of the dipole's tendency to form strong sidelobes in the forward hemisphere. The authors attributed this to the effective electrical isolation of the two hemispheres by the metallic plane containing the slot itself (Leung et al., 1997). Both experiments showed that while a PBG reflector could improve antenna radiation characteristics, a poor choice of position could actually degrade antenna performance.

Finally, first of two papers, Poilasne et al. investigated the use of a planar MPBG reflector with dipole and square spiral antennas (Poilasne et al. 1997). Their measurements of the spiral antenna's radiation showed that depending on frequency, their structure could either degrade or enhance the region over which the polarization remained circular.

They also performed a simple ray-optics analysis of a point source above a dielectric-coated reflection plane to derive two necessary and sufficient phase conditions for wideband constructive interference (Figure 1). Cast in terms of the variables used in the present work, these conditions are:

$$\frac{4\pi f d \sqrt{\epsilon_r}}{c_0} \cos(\theta_2) = -\Phi(f, \theta_2) + 2n\pi$$

$$\frac{4\pi d \sqrt{\epsilon_r}}{c_0} \cos(\theta_2) = -\frac{\partial}{\partial f} \Phi(f, \theta_2)$$

where  $d$  is the distance to the reflection plane,  $\theta_2$  is the angle of the refracted ray within the dielectric, and  $n$  is any integer. The other variables are by now self-explanatory.

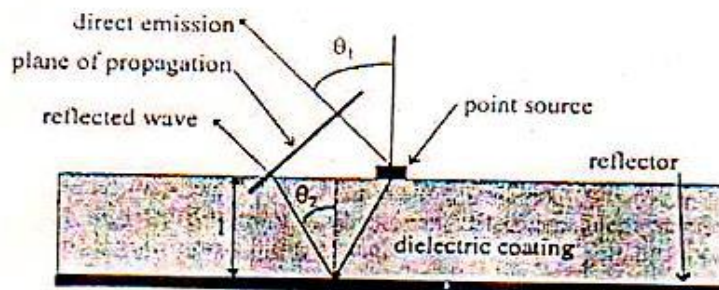


**Figure 1. Geometry for Poilasne's Reflection Plane Analysis**

Equation shows that for a given incident angle, a linearly decreasing phase presents the possibility of matching these criteria. The GTRI researchers had already observed a tendency for their PBG structure to show a linearly decreasing reflected phase within the band gap (Kesler et al., 1996). Poilasne's group showed that their reflector should also have the required linear phase behavior at normal incidence, but did not report any attempt to maximize the measured band of constructive interference.

In their second experiment, Poilasne's group altered a dipole's radiation pattern using MPBG reflectors (Poilasne et al., 1998). Compared with the beamwidth of a dipole in front of a planar PBG reflector, they increased the 3 dB beamwidth 64% by using a MPBG corner reflector. They further suggested such a configuration might be useful in suppressing grating lobes for a dipole array.

## Conclusion :

The use of PBG substrates might allow significant gain improvement for planar antennas by overcoming the problem of power loss into homogeneous substrates and wideband enhancement also appeared possible but more research is needed to resolve questions concerning both the effect of a PBG substrates on an antennas pattern- shape and the sensitivity of antenna performance to placement relative to the PBG lattice. No doubt PBG substrates and reflectors are potentially useful for improving antenna gain, efficiency and directivity.

## References :

- Agi, K., E. R. Brown, O. B. McMahon, C. Dill III and K. J. Malloy. "Design of ultrawideband photonic crystals for broadband antenna applications," Electronics Letters 30: 2166-2167 (1994).
- Brown, E. R., C. D. Parker, and E. Yablonovitch. "Radiation properties of a planar antenna on a photonic-crystal substrate," Journal of the Optical Society of America B 10: 404-407 (1993).
- Cocciali, R., W. R. Deal, and T. Itoh. "Radiation characteristics of a patch antenna on a thin PBG substrate," IEEE Antennas & Propagation Symposium Proceedings, 1998, 656-657.
- Ellis, Thomas J. and Gabriel M. Rebeiz. "MM-Wave Tapered Slot Antennas on Micromachined Photonic Bandgap Dielectrics," IEEE Microwave Theory & Techniques Symposium Digest, 1996, 1157-1160.
- Kesler, M. P., J. G. Maloney, and B. L. Shirley. "Antenna design with the use of photonic bandgap materials as all dielectric planar reflectors," Microwave and Optical Technology Letters 11: 169-174 (1996).
- Leung, K. M. "Diamondlike photonic band-gap crystal with a sizable band gap," Physical Review B 56: 3517-3519 (1997).
- Poilasne, G., J. Lenormand, P. Pouliken, K. Mahdjoubi, C. Terret, and Ph. Gelin. "Theoretical Study of Interactions Between Antennas and Metallic Photonic Band-Gap Materials," Microwave and Optical Technology Letters 15: 384-389 (1997).
- Poilasne, G., P. Pouliken, K. Mahdjoubi, C. Terret, Ph. Gelin, and L. Desclos. "Radiation Characteristics of a Half Wavelength Dipole Inside Metallic Photonic Band-Gap Structures," IEEE Antennas & Propagation Symposium Proceedings, 1998, 170-173.
- Sigalas, M. M., R. Biswas, Q. Li, D. Crouch, W. Leung, R. Jacobs-Woodbury, B. Lough, S. Nielsen, S. McCalmont, G. Tuttle, and K.M. Ho. "Dipole Antennas on Photonic Band-Gap Crystals -Experiment and Simulation," Microwave and Optical Technology Letters 15: 153-158 (1997).
- Smith, Glenn S., Morris P. Kesler, and James G. Maloney. "Dipole antennas used with all-dielectric, woodpile photonic-bandgap reflectors: gain, field patterns, and input impedance," scheduled for publication in Microwave and Optical Technology Letters (1999).

Yang, Hung-Yu David, Nicolaos G. Alexopoulos, and Eli Yablonovitch. "Photonic Band-Gap Materials for High-Gain Printed Circuit Antennas," IEEE Transactions on Antennas and Propagation 45: 185-187 (1997).

Yang, D. H. and K. Agi, Session Chairs. "Antenna Applications of Photonic-Band-Gap Materials," Special Session in USNC/URSI National Radio Science Meeting Digest. 113-123 (1998).

Yablonovitch, E. "Inhibited Spontaneous Emission in Solid State Physics and Electronics," Physical Review Letters 58: 2059-2062 (1987).

Zhang, Lijun, Harry Contopanagos, Nicolaos G. Alexopoulos, and Eli Yablonovitch. "Cavity Backed Antennas with PBG-Like Substrate or Superstrate Materials," IEEE Antennas & Propagation Symposium Proceedings, 1998, 186-189.

## Study of Pattern and Gain Properties of a Dipole Antennas

DHIRENDRA KUMAR and PRAKASH NAYAK

Department of Physics, R. K. College, Madhubani.

### Abstract

This paper examines the pattern, gain, and impedance properties of a dipole antenna located close to a high - impedance material. A high-impedance conductor with reflection coefficient magnitude near unity and appropriate phase would allow a parallel dipole to be closely spaced to the screen. The material is idealized with a unity reflection coefficient and a variable phase angle from  $0$  to  $+\pi$  and  $-\pi$ . An example uses a half-wave dipole-spaced wavelength from the material. For a phase angle around  $135^\circ$  the pattern is unstable and has a null at broadside. Gain varies from  $10$  to  $0$  dB. Input impedance varies widely with phase angle, presenting a mismatch loss situation. From these data an acceptable range of phase angle versus frequency can be inferred.

**Keywords:** Antennas, electromagnetic bandgap, high impedance screen, magnetic conductor, photonic bandgap.

### Introduction

Microwave impedance surfaces have been known for decades and have borne the names of artificial dielectrics and frequency selective surfaces. Some of these surfaces in the last few years have been called photonic bandgap (PBG) materials (Yang, 1999 and Scherer *et al.*, 1999). Other terms for these are electromagnetic bandgap material, artificial magnetic conductor, and high-impedance conductor, which apply to their use as a screen for dipole antennas. Much work has been reported on PBG materials, but for many, the reflection coefficient versus frequency is quite irregular (Agi K. *et al.*, 1994). A reflection coefficient magnitude that is close to unity and flat over a frequency range (Barlevy S. *et. al.*, 2001) is indicated for screen use. Other uses of PBG for antennas include the suppression of surface waves in patch arrays with high and/or thick substrates (Kyriazidou A., *et al.*, 2000). It is interesting to note that many years ago patch antenna practitioners simply drilled many holes in the dielectric substrate to suppress surface waves.

Other antenna applications include patch PBG superstrates to increase gain (Hansen R. C. 1998), reflect arrays, and reflectors (Thakur O. P. *et. al.*, 2012). This paper is concerned with use of a PBG screen as a high-impedance conductor to act as an antenna ground plane or screen. The advantage here is simply that such a surface, with a reflection coefficient of  $+1$ , instead of the  $-1$  produced by an electric conductor, would allow a dipole parallel to the surface to be placed close to it. Further, if the  $+1$  reflection coefficient could be maintained over a frequency band, the result would be a wide-band ground plane or screen. In cases where the reflection magnitude is unity over a band, the phase is approximately linear with frequency (Shaban, *et. al.*, 2008), but the slope has the wrong sign to make screen spacing constant in wavelengths. The dipole screen needs a non-Foster reactance variation with frequency. General conditions for the ideal  $\epsilon G = 1$  have also been given (Kandu K. G. A. *et. al.*, 2012.). To establish

performance limits, the approach here is to assume  $\epsilon G = 1$  and investigate performance versus screen phase angle. Specifically, how do the broadside directivity, pattern, and impedance of a half-wave dipole parallel to the surface vary with the reflection phase angle.

### Mathematical Derivation

A dipole parallel to a screen has a screen pattern given by

$$E_{\text{scr}} = \exp(-jkh \cos \theta) + (jz + jkh \cos \theta) \quad (1)$$

Where  $k = 2\pi/\lambda$ ,  $h$  is the dipole-screen spacing,  $\theta$  is the polar angle from normal to the screen, and  $z$  is the screen reflection coefficient phase angle. It is assumed that the reflection coefficient magnitude is unity. Equation (1) becomes

$$E_{\text{scr}} = 2 \cos\left(\frac{\zeta}{2} + kh \cos\theta\right) \quad (2)$$

A metallic screen with  $z = 180$  yields  $E_{\text{scr}} = \sin(kh \cos\theta)$ . The dipole pattern, assuming it lies along the  $x$ -axis, with the  $z$ -axis normal to the screen is

$$E_{\text{dip}} = \frac{\cos(0.5kL \sin\theta \cos\phi) - \cos(0.5kL)}{\sin^2\theta \cos^2\phi} \quad (3)$$

Where the dipole length is  $L$ . Patterns are readily calculated and are shown in Figure 1 and 2. These examples are for a half-wave dipole with a screen spacing of  $0.1\lambda$  and  $0.05\lambda$ . Here, each pattern has been normalized to  $0$  dB. Patterns are shown for  $\zeta$  from  $-180$  to  $+180$  at  $45^\circ$  steps. Note that patterns are symmetric in  $\theta$  so only  $\theta = 0$  to  $90^\circ$  are shown. Also  $z = \pm 180$  gives the same pattern. A null occurs for

$$\cos\theta = \frac{(\pi - \zeta)}{2kh} \quad (4)$$

With the  $0.1\lambda$  screen spacing, the null for  $\zeta = 135^\circ$  occurs for  $\theta = 51.32^\circ$ . For  $\zeta = +90^\circ$ , the pattern at  $0^\circ$  has a  $2.5$  dB dip. All of these patterns are for  $f = 0$ , i.e., in the plane of the dipole.

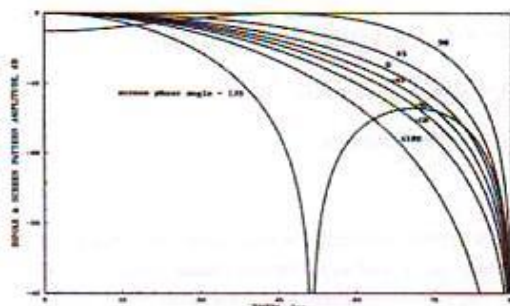


Figure 1

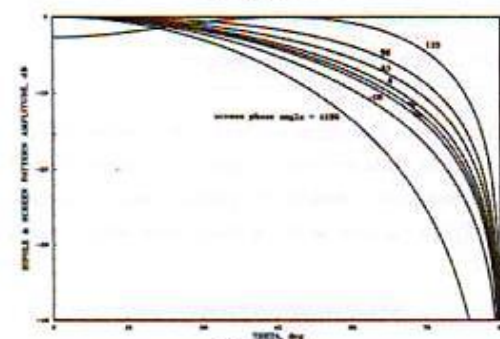


Figure 2

### Result and Discussion

A half-wave dipole is used as an example, with screen spacing's of  $0.1\lambda$  and  $0.05\lambda$ . Figure 3 shows broadside directivity versus  $\zeta$ . The value for  $\zeta = 180$  exactly checks the classical value for a conducting ground plane as does the  $\zeta = 135$ , both

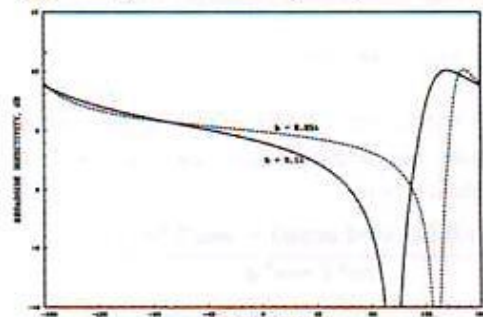


Figure 3

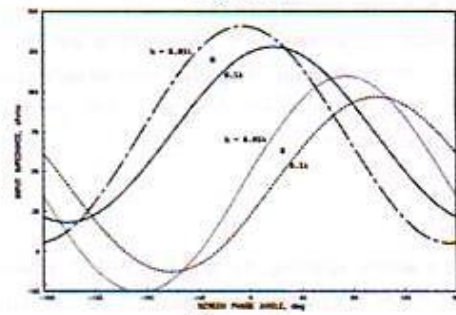


Figure 4

Using the mutual resistance formulation of directivity [20]. At  $\zeta = 108^\circ$  for  $h = 0.01$  and  $\zeta = 144^\circ$ , for  $h = 0.05\lambda$ , the pattern has a broadside null. So the directivity there is zero. The directivity peaks at  $\zeta = 153^\circ$  and  $167^\circ$  occur because the pattern main beam is narrowing but the sidelobe is still low. Input impedance is shown in Figure 4, where it may be noticed that resistance varies over a  $5:1$  range, while reactance varies over a  $4:1$  range. Thus, significant mismatch loss is experienced if the phase-angle range is large. The reflection coefficient magnitude may be less than unity due to losses and to transmission through the material. Loss will reduce the antenna efficiency and will reduce the gain. Transmission through the material will also reduce the gain (as the image radiation will be smaller), but more importantly will produce backward radiation.

### Conclusion

For a magnetic ground plane with unity magnitude of reflection coefficient, the useful range of reflection coefficient phase appears to be  $-180$  to  $+45$ . However, since a phase of  $-180$  and a close spacing produces a small net radiation resistance, the realistic range of usefulness is probably only  $\pm 45$ . A reflection coefficient magnitude less than unity will reduce gain and increase backward radiation. Of course, loss in the screen will reduce the efficiency as well.

### Acknowledgment

Authors gratefully acknowledge to U. G. C. (New Delhi) for granting a Major Research Project.

### References

1. Agi K. et al., 1994. Design of ultrawideband photonic crystals for broadband antenna applications, *Electron. Lett.*, **30**: 2166-2167.
2. Barlevy S. and Y. Rahmat - Samii, 2001. Characterization of electromagnetic band-gaps composed of multiple periodic tripods with interconnecting vias: Concept, analysis, and design, *IEEE Trans. Antennas Propagat.*, **49**: 343-353.
3. Hansen R. C. 1998. *Phased Array Antennas*. New York: Wiley.
4. Kandu K. G. A. and D.C. Dhubkarya, 2012. Enhanced bandwidth of rectangular microstrip patch antenna using Photonic Band Gap (PBG) structure, *Int. Jr. of Knowledge Engineering and Technology*, **1(1-2)**: 25 - 32.
5. Kyriazidou A., et al., 2000. Artificial versus natural crystals: Effective wave impedance of printed photonic bandgap materials, *IEEE Trans. Antennas Propagat.*, **48**: 95-106.
6. Shaban, H. F., H. A. Elmikaty, and A. A. Shaalan, 2008. Study the effects of Electromagnetic Band-Gap (EBG) substrate on two patches microstrip antenna, *Progress In Electromagnetics Research B*, **10**: 55-74.
7. Scherer A. et al., 1999. Electromagnetic crystal structures, design, synthesis, and applications, *IEEE Trans. Microwave Theory Tech.—Special Issue*, **47**: 2057-2150.
8. Thakur O. P., Dwari S and Kushwaha A. K., 2012. Enhancement of bandwidth by using photonic bandgap structure in microstrip antenna, *International Journal of Computational Intelligence Techniques*, **3(2)**: 112-113.
9. Yang, H. -Y. D. 1999. Theory and applications of photonic band-gap materials, *Electromagn.—Special Issue*, **19**: 223-335.

## Study of Photonic Bandgap Structures below Infrared Wavelengths

DHIRENDRA KUMAR and PRAKASH NAYAK

Department of Physics, R. K. College, Madhubani – 847211(Bihar)

Mail – [k.dhirendra17@gmail.com](mailto:k.dhirendra17@gmail.com)

### Abstract

Photonic bandgaps in 2- and 3- dimensional crystals are hard to achieve due to the limited contrast in the dielectric permeability available with conventional dielectric materials. The situation changes for periodic arrangements of scatterers consisting of materials with a Drude-like behaviour of the dielectric function. In this study we shows that for two-dimensional square and triangular lattices that such systems have in-plane complete photonic bandgaps (CPBGs) below infrared wavelengths. The optimal one for ideal Drude-like behaviour is a square lattice, whereas for Drude-like behaviour in silver, the geometry is a triangular lattice. If the lattice spacing is tuned to a characteristic plasma wavelength, several CPBGs open in the spectrum and their relative gap width can be as large as 38.6%. Such structures can provide CPBG structures with bandgaps down to ultraviolet wavelengths.

**Keywords:** Photonic bandgap materials, nonlinear optical materials, integrated optics, fiber waveguides, wave optics.

### Introduction

In recent years, a new technology has emerged which may be the key to developing ultra-wideband microstrip antennas. This technology manipulates the substrate in such a way that surface waves are completely forbidden from forming, resulting in improvements in antenna efficiency and bandwidth, while reducing sidelobes and electromagnetic interference levels. These substrates contain so called Photonic Crystals. Also known as electromagnetic band-gap (EBG) structures and electromagnetic band-gap materials (EBMs), are a class of periodic metallic, dielectric, or composite structures that exhibit a forbidden band, or bandgap, of frequencies in which waves incident at various directions destructively interfere and thus are unable to propagate (1, 2). Based on the dimensional periodicity of the crystal structure, the bandgaps can be in one, two, or three-dimensional planes, with the level of complexity increasing as the dimensions increase. If the periodicity in an EBG structure is perturbed by either removing or adding a material with a different dielectric constant, size, or shape, a “defect” state is created in the forbidden gap, where an electromagnetic mode is allowed, and localization of the energy occurs. For many technological applications it is enough to achieve a photonic bandgap (PBG) for in-plane propagation and, for applications involving highly polarized light sources, it can be sufficient to obtain a PBG for a single polarization only. We know that

for in-plane propagation, the two photon polarizations do not mix and Maxwell's equations reduce to two scalar equations, one for each polarization. Numerous applications have been suggested involving two-dimensional (2D) photonic structures, i.e. new designs for light-emitting diodes([3,6], polarizers (4,7), high transmission through sharp bends (5,8), efficient bandpass filters, channel drop filters, and, in one dimension, waveguide crossing without cross-talk (6, 9). We shall focus only on 2D photonic structures. For such structures, only an in-plane CPBG can ensure light propagation control whatever the in-plane light propagation. Fabrication of photonic crystals with such a gap poses a significant technological challenge for 2D structures already in the near-infrared (10), not to mention three-dimensional (3D) photonic structures (11).

A 2D photonic crystal can be thought of as a 2D periodic arrangement of scatterers with a dielectric constant  $\epsilon_s$  embedded in a host with a dielectric constant  $\epsilon_h$ . In view of the scale invariance present in Maxwell's equations it makes sense to introduce the relative gap width  $g_w$  as the gap width-to-midgap frequency ratio,  $\nabla\omega/\omega_m$ . Practical crystals are expected to have  $g_w$  larger than a few percent—to leave a margin for gap-edge distortions due to omnipresent impurities and yet to have a CPBG useful for applications. We only discuss square and triangular lattices of infinitely long cylindrical scatterers with circular cross section and with one cylinder per lattice unit cell. Even then,

for instance in a 2D square lattice of cylinders for a cylinder filling fraction of 65% in a silica host (figure 1), several CPBGs open, one of them larger than 11.4% and another larger than 35%, provided that cylinders are made out of material with a Drude-like dielectric function.

$$\epsilon_s(\omega) = 1 - \frac{\omega_p^2}{\omega^2} \quad (1)$$

Where  $\omega_p$  denotes the plasma frequency. The Drude-like dielectric function is zero for  $\omega = \omega_p$  which makes  $\delta$  infinite and enables one to avoid the restrictions on the dielectric contrast. This approach has been shown to also work for 3D photonic structures. The proposed structures could be realized by introducing, for instance by electrochemical deposition, a Drude-like material into the holes of a periodic structure of air holes in a dielectric, a structure that has no CPBG without the Drude-like material inserted into the holes of a periodic structure of air holes in a dielectric, a structure that has no CPBG without the Drude-like material inserted (figure 1).

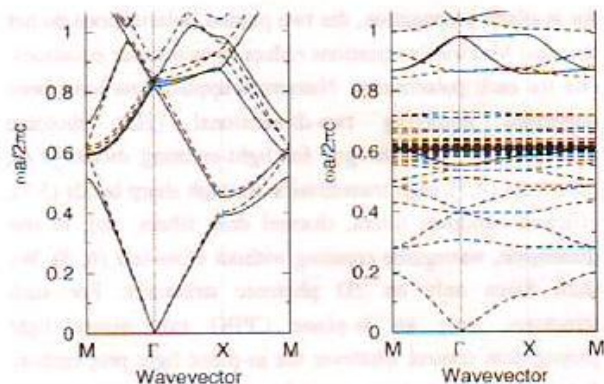


Figure 1(a) and 1(b)

Metals can be quite lossy at optical frequencies. Nevertheless, the absorption can be rather small in a certain frequency window, where the metal behaves as a highly dispersive dielectric. The plasma wavelength  $\lambda_p = \frac{2\pi c}{\omega_p}$ , where  $c$  is the speed of light in vacuum, is closer to the short-wavelength edge of the nonabsorptive window, since for shorter wavelengths there is a higher probability of inducing electronic interband transitions. We restricted our investigation mainly to the 'nonabsorptive' window for the ideal Drude behaviour; 310–520 nm for silver (15). We studied both square and triangular lattices, the Bravais lattices that have Brillouin zones that come closest to a circle, and are hence expected to give rise to the biggest

bandgaps. We find that for an ideal Drude-like material a square lattice leads to the biggest gaps of the two lattice types studied. However, the deviation of the dielectric function of silver from the ideal Drude behavior means that silver triangular lattices result in bigger CPBGs than square lattices. In both cases, i.e. ideal Drude/square and silver/triangular, a CPBG with  $g_\omega \approx 10\%$  is even found for a host dielectric constant  $\epsilon_h$  as low as  $\epsilon_h = 1$ .

### Method and Discussion

We performed band-structure calculations using a 2D analogue of the familiar Korringsa–Kohn–Rostocker (KKR) method. Since, for in-plane propagation, the two photon polarizations decouple, the calculation reduces to the use of the ordinary 2D scalar KKR method (14) for either polarization. This polarization decoupling is specific to two dimensions and is obviously not the case for 3D photonic structures where a truly vectorial KKR method is required. Given a plasma frequency  $\omega_p$ , we performed calculations for frequencies from  $\approx 0.5 \omega_p$  to  $1.1 \omega_p$ , assuming  $\epsilon_h$  is constant in this frequency region. In contrast to the plane-wave method (4, 7), dispersion does not cause any difficulties for the KKR method and the computational time is the same as without dispersion. The qualitative behaviour of the band structure for a 2D periodic arrangement of Drude-like scatterers is similar to that in three dimensions (13). The plasma wavelength sets a characteristic scale and, correspondingly, bandgaps only occur for certain values of  $r_c/\lambda_p$  or  $a/\lambda_p$  where  $r_c$  and  $a$  are the cylinder radius and lattice constant, respectively. Of the two geometries studied, a square lattice is optimal for a Drude metal. Besides the CPBGs mentioned above, we also found very large CPBGs at lower frequencies, outside the 'nonabsorptive' window, typically at midgap frequencies of 20% of the plasma frequency. For instance, in the case of the structure presented in figure 1(b) for  $\epsilon_h = 2.16$ , we found a CPBG with  $g_\omega = 35\%$ , at  $\omega_m/\omega_p = 0.217$  ( $g_\omega = 36.9\%$  at  $\omega_m/\omega_p = 0.213$  for  $\epsilon_h = 1$ ). For a triangular lattice one encounters more CPBGs. However, the maximal found was  $g_\omega = 3.5\%$ . For silver we used the experimental data from Palik. The deviation from the ideal Drude behaviour, which occurs in the proximity of the zero-crossing of  $\text{Re } \epsilon$  at  $\lambda_c = 328$  nm (13), means that for silver a triangular lattice leads to bigger CPBGs than a square lattice (Figure 2).

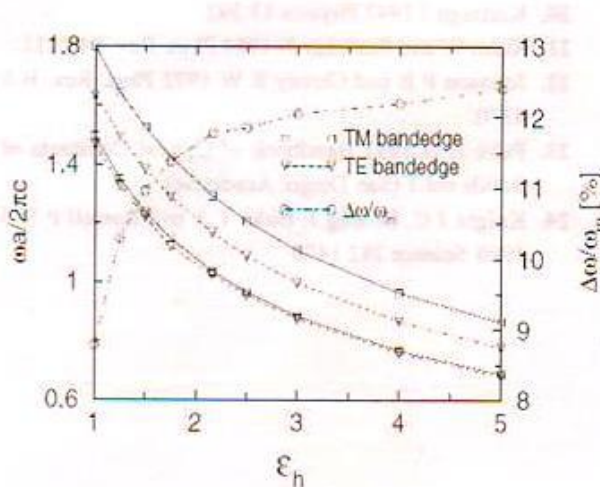


Figure 2

Our aim was to show that practical in-plane CPBGs can open for the simplest 2D lattice and scatterer geometries, as long as the scatterer dielectric function is correctly chosen. Our proposal in using scatterers with a metallic Drude-like dielectric function (1) offers a new and promising way to fabricate 2D structures with a practical CPBG in the wide frequency range from GHz to ultraviolet. A typical plasma frequency of a metal is in the ultraviolet, whereas that of a semiconductor is in the infrared. On the other hand, it has been shown that a whole new class of artificial materials can be fabricated in which the plasma frequency may be reduced by up to six orders of magnitude compared with conventional materials, from UV down to GHz frequencies. Correspondingly, the proposed structures can provide CPBG structures in this frequency range.

The observed magnitude and robustness of the in-plane CPBG of the metallo-dielectric structures allows one to speculate that an inclusion of metallic (silver) wires could also boost the performance of the photonic crystal fibre designed by Knight *et al.* The photonic crystal fibre is a 2D photonic periodic arrangement of thin cylindrical glass fibres where the light is sent along the cylinder axis.

In lateral directions, the localization of light is achieved in complete analogy to the case of electrons: it is possible to introduce a defect at the centre of the photonic crystal fibre, for instance by omitting one cylinder, such that it induces a transversely localized mode with frequency within a 2D CPBG. The lights can then propagate with that frequency along the cylinder axis even if the core of the photonic crystal fibre is air and if the cladding has a higher refractive index.

## Conclusion

We have shown that one can achieve a relative gap width  $g_\omega$  larger than 10%, one expects that the width can be enlarged further by more than one scatterer per unit cell. We also point out that the idea of using highly dispersive metallic and semiconductor components for photonic structures is not new (7, 16). Calculations using the plane-wave method (2) have often been restricted to an extremely low filling fraction  $f \leq 1\%$ , of metallic components (7). In addition, the main interest was in microwave or even in radiofrequency applications. Surprisingly enough, no systematic search has been made for CPBGs with a Drude-like behaviour (1) of the dielectric function. There have been many studies involving 2D structures since the pioneering work of Maradudin and collaborators (4). However, these mostly require unrealistic values of the dielectric contrast  $\delta$  to produce a CPBG below infrared wavelengths.

## References

1. Yablonovitch E 1987 Phys. Rev. Lett. 58 2059.
2. Ho K M, Chan C T and Soukoulis C M 1990 Phys. Rev. Lett. 65 3152.
3. Yablonovitch E, Gmitter T J and Leung K M 1991 Phys. Rev. Lett. 67 2295.
4. Plihal M, Shambrook A, Maradudin A A and Sheng P 1991 Opt. Commun. 80 199.
5. Plihal M and Maradudin A A 1991 Phys. Rev. B 44 8565.
6. Yablonovitch E, Gmitter T, Meade R, Rappe A, Brommer K and Joannopoulos J D 1991 Phys. Rev. Lett. 67 3380.
7. Bykov V P 1972 Sov. Phys.-JETP 35 269.
8. Bykov V P 1975 Sov. J. Quantum Electron. 4 861.
9. Fan S, Villeneuve P R, Joannopoulos J D and Schubert E F 1997 Phys. Rev. Lett. 78 3294.
10. Boroditsky M, Krauss T F, Cocciali R, Vrijen R, Bhat R and Yablonovitch E 1999 Appl. Phys. Lett. 75 1036.
11. McGurn A R and Maradudin A A 1993 Phys. Rev. B 48 17 576.
12. Kuzmiak V, Maradudin A A and Pincemin F 1994 Phys. Rev. B 50 16 835.
13. Mekis A, Chen J C, Kurland I, Fan S, Villeneuve P R and Joannopoulos J D 1996 Phys. Rev. Lett. 77 3787.
14. Villeneuve P R, Fan S and Joannopoulos J D 1996 Phys. Rev. B 54 7837.

DHIRENDRA KUMAR and PRAKASH NAYAK

15. Fan S, Villeneuve P R, Joannopoulos J D and Haus H A 1998 *Phys. Rev. Lett.* 80 960 Johnson G, Manolatou C, Fan S, Villeneuve P R, Joannopoulos J D and Haus H A 1998 *Opt. Lett.* 23 1855.
16. Krauss T F, De la Rue R M and Brandt S 1996 *Nature* 383 699.
17. Lin S Y *et al* 1998 *Nature* 394 251.
18. Barra A, Cassagne D and Jouanin C 1998 *Appl. Phys. Lett.* 72 627
19. Drude P 1900 *Ann. Phys., Lpz.* 1 566 Drude P 1900 *Ann. Phys., Lpz.* 3 369-398.
20. Korringa J 1947 *Physica* 13 392.
21. Kohn W and Rostoker N 1954 *Phys. Rev.* 94 1111.
22. Johnson P B and Christy R W 1972 *Phys. Rev. B* 6 4370.
23. Palik E D 1991 *Handbook of Optical Constants of Solids* vol 1 (San Diego: Academic).
24. Knight J C, Broeng J, Birks T A and Russell P St J 1998 *Science* 282 1476